

April 2012

Dynamic Evaluation of Forces During Mastication

Anthony George Spangenberg
Worcester Polytechnic Institute

Justin Ochoa McGarry
Worcester Polytechnic Institute

Follow this and additional works at: <https://digitalcommons.wpi.edu/mqp-all>

Repository Citation

Spangenberg, A. G., & McGarry, J. O. (2012). *Dynamic Evaluation of Forces During Mastication*. Retrieved from <https://digitalcommons.wpi.edu/mqp-all/95>

This Unrestricted is brought to you for free and open access by the Major Qualifying Projects at Digital WPI. It has been accepted for inclusion in Major Qualifying Projects (All Years) by an authorized administrator of Digital WPI. For more information, please contact digitalwpi@wpi.edu.



Project Number: ME-SYS-0787

Dynamic Evaluation of Forces During Mastication

A Major Qualifying Project
Submitted to the Faculty of
WORCESTER POLYTECHNIC INSTITUTE
In partial fulfillment of requirements for the
Degree of Bachelor of Science

By

Justin McGarry

Anthony Spangenberger

Date:

Approval:

Professor Satya Shivkumar, Advisor

Abstract

A reproduction of the human masticatory system is presented here to evaluate mechanical properties of foods, relevant design elements of the simulator, and the overall practicality of the system. The model incorporates a cam-driven linkage system providing realistic motion of the mandible, with reaction forces measured by strain gages on two axes to record real time changes in food structure. The experiment demonstrates that the construction of a mastication simulator is feasible and allows texture profiling and discrimination between similar foods.

Acknowledgements

Our MQP was completed with the help of several individuals who offered professional advice and technical guidance. We would like to thank Prof. Satya Shivkumar, our project advisor, for guiding us with his extensive knowledge of materials and testing procedures, Prof. John Hall for his help with the sensors used in this project and his willingness to lend some of the necessary equipment, Prof. Robert Norton for his advice on the fixture design, Fred Hutson for lending equipment from the physics department for use in calibration of the fixture, Randy Robinson for the computer used for recording data, Neil Whitehouse, Toby Bergstrom, and Adam Shears for their support in machining, and Maximilian Kaiser for the use of his tools.

Contents

Abstract.....	i
Acknowledgements.....	ii
Table of Figures.....	iv
Table of Tables.....	v
1.0 Introduction.....	1
2.0 Background.....	3
2.1 Muscles of Mastication.....	3
2.2 Human Bite Force.....	4
2.3 Review of Mastication Simulators.....	5
2.3.1 Teeth.....	5
2.3.2 Force Measurement.....	7
2.3.3 Texture Profile Analyzers.....	8
3.0 Objectives.....	11
4.0 Fixture Design.....	12
5.0 Methodology.....	23
5.1 Fixture Calibration.....	23
5.2 Sample Preparation.....	23
5.3 Sample Testing.....	23
5.4 Data Analysis.....	23
6.0 Journal Paper, Design of a Fixture for the Dynamic Evaluation of Forces During Mastication.....	25
7.0 Journal Paper, Dynamic Evaluation of Texture in Chocolate.....	34
8.0 Conclusions.....	42
9.0 Works Cited.....	44
10.0 Appendix.....	47
10.1 Brittle Foods.....	48
10.2 Highly Viscoelastic Foods.....	50
10.3 Lightly Viscoelastic Foods.....	52
10.4 Sample Masses.....	58

Table of Figures

Figure 1. The principal muscles involved in mastication.....	3
Figure 2. The principal motions involved in mastication.....	3
Figure 3. Numbering of adult human teeth.....	4
Figure 4. Body planes used for describing reference locations.....	4
Figure 5. The JSN/2A jaw simulator device constructed at the Niigata University, Japan.....	6
Figure 6. The 6 RSS parallel mechanism.....	6
Figure 7. Dual molar mastication robot with components labeled.....	6
Figure 8. The WJ-3 robot that uses a human skull model and artificial muscle actuators.....	7
Figure 9. A simple gnathodynamometer.....	7
Figure 10. A typical strain gauge, enlarged for detail.....	8
Figure 11. Mounting of maxilla.....	12
Figure 12. 1 DOF systems.....	13
Figure 13. 2 DOF systems.....	13
Figure 14. Pivoting linkage design.....	14
Figure 15. Crossed linkage design.....	14
Figure 16. Pinion-driven rotary cams.....	14
Figure 17. Linear cams.....	15
Figure 18. A cam-linkage system.....	15
Figure 19. Another cam-linkage system.....	16
Figure 20. Double-translating linkages.....	16
Figure 21. Symmetrical double-translating linkages.....	16
Figure 22. Early strain gage mounting concept.....	17
Figure 23. Support mounted strain gages.....	17
Figure 24. Fixing supports of the base.....	18
Figure 25. Base plate.....	18
Figure 26. Modeled cam and cam mounting.....	19
Figure 27. Modeled linkages, base plate, and jaws.....	19
Figure 28. Manufactured fixture in Instron.....	21

Table of Tables

Table 1. Maximum bite force of male and female subjects as reported by other articles.....	5
Table 2. Parameters defined by Szczesniak for Texture Profile Analysis.....	9
Table 3. Positions of the cam over time.....	20

1.0 Introduction

A mastication simulator is any device that reproduces the conditions present during the process of chewing in order to reconstruct the complicated process of mastication outside the body. Typically, the device consists of an actuating surface that reproduces the motions and/or forces observed in mastication. Attempts can also be made to replicate chemical, thermal, and additional physiological features depending on the desired accuracy and experimental outcome. (Salles, et al., 2007) (Kawashima, Miura, Kato, Yoshida, & Tanaka, 2009) The end result is a device that allows the user to observe the complicated process of mastication without obfuscation by adjacent tissues (cheeks, tongue, lips, etc.). A simulator also produces more consistent results on a test-by-test basis than human subjects in situations where *in vivo* data is not necessitated. (Villamil, Nedel, Freitas, & Maciel, 2005)

The desired experimental outcomes include the evaluation of the relevant design criteria of a functional mastication simulator, measurement of material properties of a variety of foods, and determination of the potential for use of a simulator in industrial texture measurement. Within the food industry, texture analysis is of critical importance because it can be quantified to evaluate product quality. (Mochizuki, 2001) The desire to differentiate a product from competitors' leads food engineers to identify measurement techniques that can detect desirable qualities in the texture of foods. For example, in commercial manufacturing of white bread, engineers strive to maximize hysteresis of the product because of superior reception of this characteristic that has been observed among consumers. Food properties as measured by a mastication simulator are also of interest to materials scientists for the development of new metrics for evaluating food. Compared to standard tension/compression testing, this simulator simultaneously combines compressive and shear forces that are present during human mastication. In this way it is possible for a simulator to produce information where more generalized techniques fall short. It will be shown that the mastication simulator described here compares favorably with other similar devices and the biological mechanism it models.

Mastication simulation is a useful tool in several areas including commercial, educational, and research applications. The significance of food texture in the food processing industry mandates the use of measurement techniques to evaluate food properties. Most industrial measurement techniques use a probe of a particular geometry (cylinder, cone, ball, etc.) to analyze how the food responds to an applied force. (Texture Technologies, 2011) Using a device to reproduce human mastication eliminates the variable of geometry and directly analyzes the human response to the food instead of intermediate measurements. Therefore more accurate data can be gathered regarding how the food is perceived rather than of the food itself. As an educational tool a mastication simulator can be used as an aid in dentistry education by reproducing motions of the chewing process obfuscated by the tongue and cheeks. (Tanzawa, et al., 2011) Many properties that cannot be observed or measured adequately during mastication can be better understood by replicating the process externally.

A device simulating particular aspects of mastication is especially useful in research applications when a probe cannot be inserted into the body. A mastication simulator is not limited to the measurement of food properties as described here; they have also been applied to measure wear

properties of teeth (Mello, Coppede, Macedo, Chiarello de Mattos, Rodrigues, & Ribeiro, 2009), to evaluate characteristics of denture materials (Conserva, et al., 2008) and (Conserva, et al., 2009), and to characterize food bolus formation (Woda, et al., 2010). Mastication simulators as a tool are incredibly versatile because they can be designed based on different criteria to emphasize relevant features. For this application, it is desirable to reproduce the geometry of both the mouth's motion during mastication and that of the teeth in order to dynamically observe the forces produced by foods. This is accomplished by first reviewing the relevant criteria that affect masticatory motions, human bite force, and similar devices.

2.0 Background

2.1 Muscles of Mastication

Human mastication is an elegant interaction of several muscle groups that is subconsciously refined into a simple process by repetition. More than twenty muscles are responsible for the motion profile, which is considered to be an aggregate of both clenching and grinding motions. (Daumas, Xu, & Bronlund, 2005) In many simulations the complex muscular interplay is simplified to the principal three muscles involved in mastication: the temporal, the masseter, and the pterygoid muscles. [(Daumas, Xu, & Bronlund, 2005) and (Conserva, et al., 2008) and (Takanbu, Takanishi, & Kato, 1993) and (Takanobu, Yajima, Nakazawa, Takanishi, Ohtsuki, & Ohnishi, 1998)] These four muscles are pictured in Figure 1.

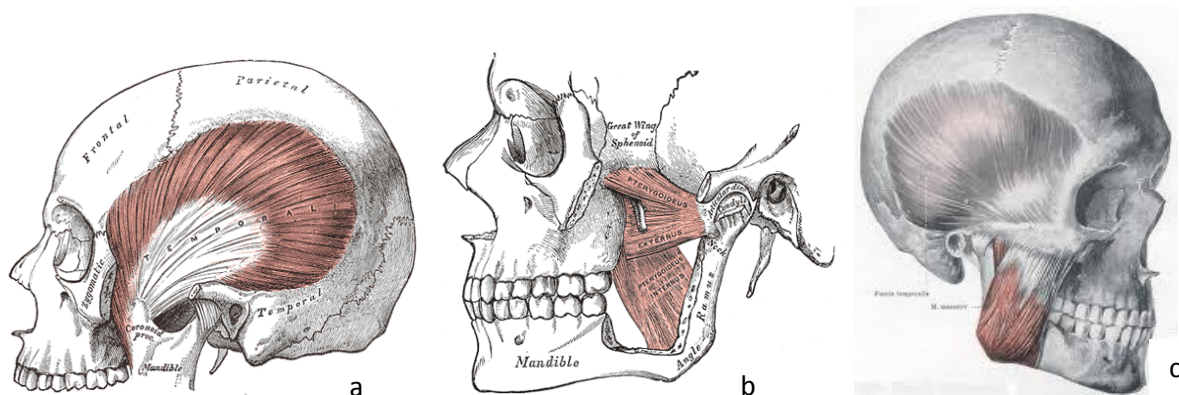


Figure 1. The principal muscles involved in mastication, a) the temporal, b) the pterygoid internus and externus, and c) the masseter.

The function of the temporal muscle is to elevate the mandible and also retract it by activation of posterior fibers. The pterygoid muscles serve to depress the mandible (externus), elevate the mandible (internus), and both groups are used to produce lateral excursions of the mandible. Much of the masticatory force is produced by the masseter, which can elevate and protrude the mandible. The combined actions of these muscles produce the motion profiles shown in Figure 2.

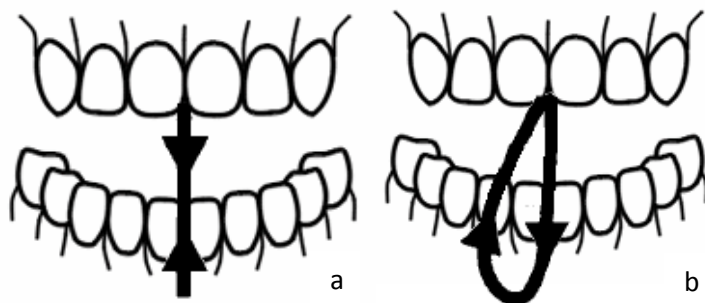


Figure 2. The principal motions involved in mastication, a) clenching and b) grinding.

Clenching is the vertical motion of the jaw that involves shearing of the food at the incisors and compression of the food at the molars. Grinding is a combination of compression and shear force

application at the molars. Both of these motions may also put any food that sticks to the teeth in tension due to adhesion as the occlusal surfaces separate.

It is also necessary to define established reference points that refer to specific teeth and body planes. For teeth numbering, customary notation using the Universal Numbering System is employed for permanent adult teeth with third molars. A diagram indicating the reference number for each tooth is shown in Figure 3. Three reference planes are also employed to differentiate locations of the body and relative motion between two body parts. These planes are well established anatomical references that have been established by the Federative Committee on Anatomical Terminology and are used

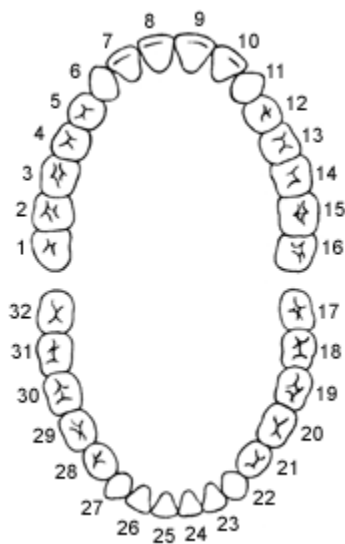


Figure 3. Numbering of adult human teeth.

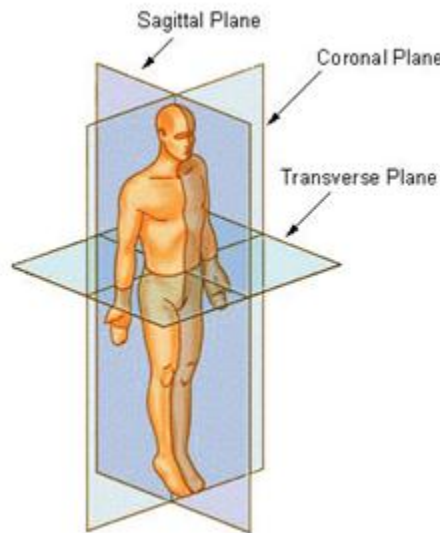


Figure 4. Body planes used for describing reference locations.

internationally. (Terminologia Anatomica, 1998) The reference planes are known collectively as the body planes and include the sagittal plane, the coronal plane, and the transverse plane, and are depicted in Figure 4. The sagittal plane extends from the front to the rear, dividing left and right; the coronal plane separates front and back (ventral and dorsal) sections; and the transverse plane is horizontal, differentiating top and bottom sections.

2.2 Human Bite Force

Maximum human bite force and the factor that affect it have been closely studied in numerous laboratory experiments. It varies with several factors including subject gender and age, food type, jaw disorders, tooth quality, muscular strength, and other factors. Osborn reports five criteria that increase the maximum bite force independent of the subject being tested. The factors that increase force are (i) tilting the bite force forward, (ii) keeping the jaw perpendicular to the occlusal plane as it is opened, (iii) placing teeth nearer the midline, (iv) raising teeth height for forward bite forces, and (v) tilting the articular surface of the condyle forward. (Osborn, 1996) Bite force is also dependent on the teeth that are in direct contact with the food. Incisors are located in the front of the jaw and have the least mechanical advantage, being at the front of the mouth. Conversely, molars at the rear, have the greatest potential for mechanical advantage and have evolved to compress food between occlusal surfaces and shear food during grinding motions. It has been reported that the average bite force of

incisors is 40% that of molars and chewing force at the incisor is 47% of the force on molars. (Helkimo & Ingervall, 1978)

Force measurement has been conducted to assess both the force required for mastication and maximum bite force. Common foods such as carrots, biscuits, and cooked meats produce forces in the range of 70-150 N on a single tooth. (Anderson, 1956) Forces on all contacting teeth during mastication range between 190 and 260 N. (Gibbs, et al., 1981) Maximum bite force is variable between experiments, but generally falls within the range of 500-700 N. (G.D. & Williams, 1981) Maximum bite force as reported by several different articles for young, healthy subjects is shown in Table 1. It is believed that the sensation of pain limits the maximum bite force of individuals by blocking inhibitory pathways between the peridontium and elevator motoneurons. (Orchardson & MacFarlane, 1980) This has been studied in experiments where a local anesthetic is applied to the biting teeth, resulting in increased maximum bite force. (Van Steenberghe & de Vries, 1978)

Table 1. Maximum bite force in male and female subjects as reported by different articles.

Article Number	Male Max. Force (N)	Female Max. Force (N)	Measurement Device	Citation
1	847	597	Quartz force transducer	(Waltimo & Könönen, 1993)
2	909	777	N/A	(Waltimo & Könönen, 1995)
3	652	553	Strain gauge mounted on mouthpiece	(Van Der Bilt, Tekamp, Van Der Glas, & Abbink, 2008)
4	587	425	Digital dynamometer	(Calderon, Kogawa, Lauris, & Conti, 2006)
5	505	315	Digital dynamometer	(Regalo, et al., 2008)
Average	700	533	-	-

2.3 Review of Mastication Simulators

Experiments have been conducted using masticatory simulators for the better part of the last century for a range of purposes. Not only for the purpose of food texture evaluation, they have also been designed for training dental students, evaluating properties of teeth, and jaw simulation. By emphasizing different components researchers can focus on a particular aspect of the complicated jaw system. Because this report is concerned with studying forces and food properties during mastication, the significant characteristics include the fixture design, motion profiles, tooth properties, and data acquisition.

2.3.1 Teeth

The teeth used in other masticatory simulations include simulated teeth made from artificial materials, dentures, and real teeth. One study describes the use of a mastication robot to evaluate the ability of three materials (acrylic resin, composite resin, and glass composite) to resist stress. (Conserva, et al., 2008) The experiment is not concerned with the forces of actual mastication so geometry is unimportant and rounded pegs are substituted. The teeth are fixed by placing them on a pin with a

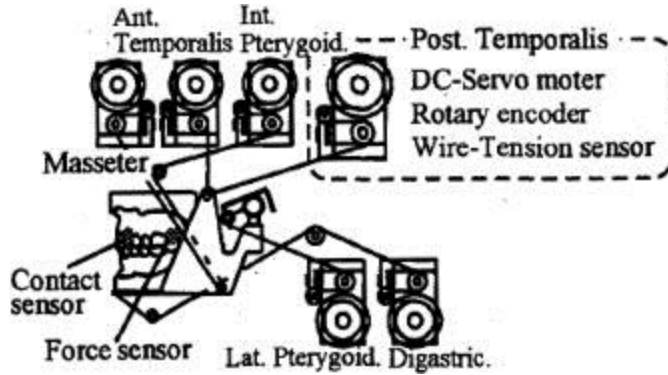


Figure 5. The JSN/2A jaw simulator device constructed at the Niigata University, Japan.



Figure 6. The 6 RSS parallel mechanism

groove that corresponds to a ridge on the inside of the sample. The results of the investigation show that the elastic modulus of the material significantly effects transmission of the force to the mastication robot, where a higher modulus corresponds to a greater maximum force. Another paper corroborates this result by demonstrating up to 63.03% greater transmission in ceramic crowns over composites. (Conserva, et al., 2009) It is concluded that greater shock absorption in the composite material is responsible for the difference in force transmission.

A simple model incorporating dentures was designed in the 1990s by using six linear actuators to represent the major muscles and simulate muscular compliance with a feedback mechanism. (Hayashi, Kato, Nakajima, Yamada, & Kobayashi, 1999) Occlusal position and force are both measured (by means of a rotary encoder and bite force sensor, respectively) and compared with the driving signal to modulate cable tension. This system is shown in Figure 5. A more recent model utilizing dentures is designed with six parallel RSS linkages each driven by a DC motor. (Torrance, Pap, Xu, Brolund, & Foster, 2006) The motion is controlled by computer (DCM-1860 control card by Galil) and motor torque is limited so as to produce a 250 N biting force at the attachment point of the link. The robot is tested by inserting a 6 mm thick aluminum plate between the upper and lower teeth to test the trajectory and the force limiting capability. This device is pictured in Figure 6.

Real teeth are clearly the most realistic material in terms of accurately reproducing the forces generated in the human mouth, and several studies have already been conducted using them. One

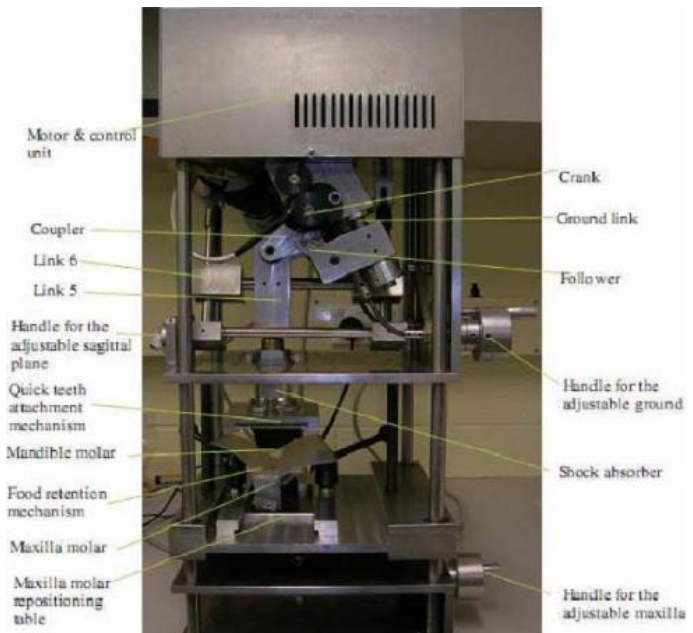


Figure 7. Dual molar mastication robot with components labeled.

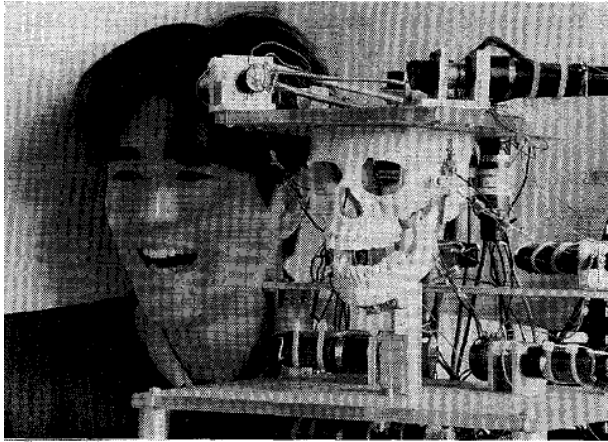


Figure 8. The WJ-3 robot that uses a human skull model and artificial muscle actuators.

Figure 8. The same fixture was later updated as the WJ-3RIII for the evaluation of masticatory efficiency. (Takanobu H. , Yajima, Nakazawa, Takanishi, Ohtsuki, & Ohnishi, 1998) The artificial muscle actuators (AMAs) developed by the group incorporate a DC motor, an encoder, a tachogenerator, a tendon, and a strain gauge force sensor. Nine of these are attached to the new model to represent two masseter, two temporal anterior, two temporal posterior, two pterygoid, and one to open the mandible. The conclusion of the experiment shows that masticatory efficiency is higher with a grinding motion as opposed to clenching.

2.3.2 Force Measurement

Measurement of masticatory force has been performed in a variety of ways dependent on the desired accuracy. To make *in vivo* measurements a device known as a gnathodynamometer (or occlusometer) is used. (Ortuğ, 2002) This generally consists of a spring-loaded mechanical device with two plates that the patient bites down on and the consequent deflection corresponds to a particular force based on calibration of the device, an example of which is shown in Figure 9. Another morphology of this device is simply a metal plate of known strength that the subject bites on, where force corresponds to the deformation of the plate. (Martin, 1997) A similar product is a pressure-sensitive film consisting of two layers of plastic, the transfer and developer sheet. (Pressurex, 2012) The transfer sheet contains microcapsules of dye that rupture at a given pressure intensity and the developer sheet captures the image with a color scale similar to Litmus paper. However, mastication robots have been used for this purpose because these other techniques are usually insufficient in terms of accuracy. (Kamegai, et al.,

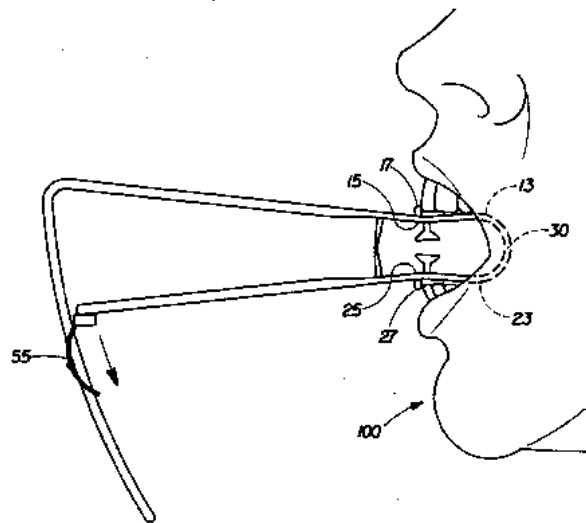


Figure 9. A simple gnathodynamometer.

2005) The tools tend to interfere with the subject's normal mastication pattern and measurements are further impeded by the addition of food.

To make accurate measurements of mastication forces it is necessary to use a simulation tool that can make dynamic measurements. The tools that have been used to make this evaluation are generally strain gauges and load cells in many mastication devices. (Conserva, et al., 2008) and (Sun, Brolund, Huang, Morgenstern, & Xu, 2008) and (Takanobu H., Yajima, Nakazawa, Takanishi, Ohtsuki, & Ohnishi, 1998) and (Conserva, et

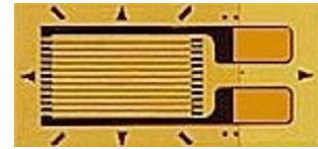


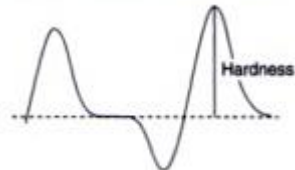
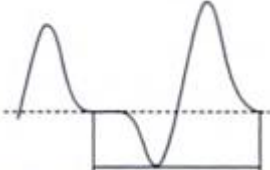
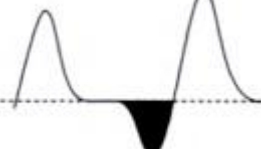
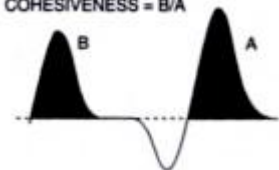
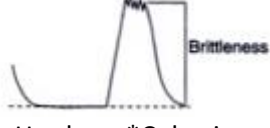
Figure 10. A typical strain gauge, enlarged for detail.

al., 2009) The strain gauge is a flexible resistor that measures strain of the substrate it is attached to based on change in area of the resistor when it deforms. An example of a typical strain gage is shown in Figure 10. A load cell is an assembly of strain gauges that is used for the measurement of force, based on a conversion from strain to stress via the elastic modulus. These devices are typically applied by forming a Wheatstone bridge, an electrical circuit used to measure small differences in resistance. Because the resistance of the strain gauge is variable, the Wheatstone bridge can be used to dynamically evaluate the resistance and corresponding strain.

2.3.3 Texture Profile Analyzers

The concept of texture profile analysis (TPA) of foods was first introduced by Szczesniak in the 1960s in an attempt to correlate human sensory analysis with empirical data from a texturometer. (Szczesniak, Brandt, & Friedman, 1963) Testing consists of a two-cycle process where a flat plunger compresses the food at 108 cm/min to 75% deformation once per cycle. Food is allowed to adhere to the plunger during testing, as the adhesive forces are an important feature of the resultant force-time curve. The data is evaluated according to seven parameters established during the study that attempt to quantify various elements of texture. These parameters are described in Table 2. It was concluded that sensory characteristics and TPA measurements did not share a linear relationship, as a consequence of undetermined variables including temperature and saliva effects. Although inconclusive in relating measurable and sensory characteristics, this experiment spurred similar studies that delved further into food texture.

Table 2. Parameters defined by Szczesniak for Texture Profile Analysis.

Parameter	Sensorial Description	Instrumental Definition
Hardness	Force required to compress food between molars	
Elasticity	The extent to which a compressed food returns to its original size with force removed	
Adhesiveness	The work required to pull the food away from a surface	
Cohesiveness	The strength of the internal bonds making up the food	$COHESIVENESS = B/A$ 
Brittleness	The force at which the food fractures	
Chewiness	The energy required to chew a solid food until it is ready for swallowing	$=Hardness * Cohesiveness * Elasticity$
Gumminess	The energy required to disintegrate a semisolid food so that it is ready for swallowing	$=Hardness * Cohesiveness$

Szczesniak later looked at the texture of gelatin and carrageenan gels under temperature variations from 20 to 30°C. (Rosenthal, 1999) She showed that hardness of gelatin decreased dramatically over the temperature range, as a consequence of melting. Carrageenan gels, which did not melt, decreased only slightly in hardness. Cohesiveness of the two gels were found to be indistinguishable across the temperature gradient. Other studies influenced by the work of Szczesniak include that of Bourne, where an Instron Universal Testing Machine is used in place of a texturometer. Using the same parameters defined by Szczesniak's 1963 study, Bourne demonstrated a decline in parameters of pears during ripening. (Bourne, 1968) Bourne concluded that these individual measurements could be correlated with a simple puncture test indicative of the overall texture.

In 1971 an experiment by Henry et al. using TPA on semisolid foods attempted to develop new parameters that related to the food's behavior during the upstroke of the plunger. (Henry, Katz, Pilgrim, & May, 1971) A sensory panel was used to rate each food based on 15 given parameters that described

the texture. Correlation analysis showed that of the 15 sensory parameters, only four were necessary to account for the variance between foods and describe each of them. Each of these four sensory parameters also correlated well with instrumental measurements. By performing multiple regressions with the data, it was found that of the 15 measureable instrumental parameters, only 8 are necessary to describe the four sensory factors. This outcome suggests that the majority of the information generated by TPA is redundant, as it is also described by other parameters.

3.0 Objectives

- Research existing methods for measuring bite force and material properties in mastication.
- Simulate the motion of chewing with the incorporation of a fixture which follows the geometry and kinematics encountered in the human mastication cycle, and record relevant forces over the duration of this cycle for specific samples of foods.
- Analyze sensory data to determine material properties and compare results to other methods that measure these properties.
- Evaluate the effectiveness of the fixture in measuring forces on different types of food samples.

4.0 Fixture Design

The procedure in this section follows four primary constraints, defined after background research and prior to any design decisions. First, the design should replicate motion of the mandible as accurately as possible (See background for a description of the human jaw's motion). Second, the device shall be driven by the Instron 4201. The use of the Instron has several advantages, including constant velocity input, feedback related to the mechanical efficiency of the fixture, and compliance with the project advisor's request for its use. Third, the device shall be able to measure shear and normal forces on the sample continuously during a test. Fourth, motion will be restricted to the Sagittal plane, as this is all that is necessary for measurement of normal and shear forces.

Producing a device which replicates the motion of a human jaw requires that the device must be capable of providing that kind of motion. First, types of motion were divided based on the degrees of freedom available to the mandible's motion. Nearly all of the designs shown later in this section have a single degree of freedom when viewed as a system, but first, only the kinds of motion available to the mandible itself will be considered. Choosing between these options is a compromise between simplicity of design, repeatability between tests, and realism in the motion of the device.

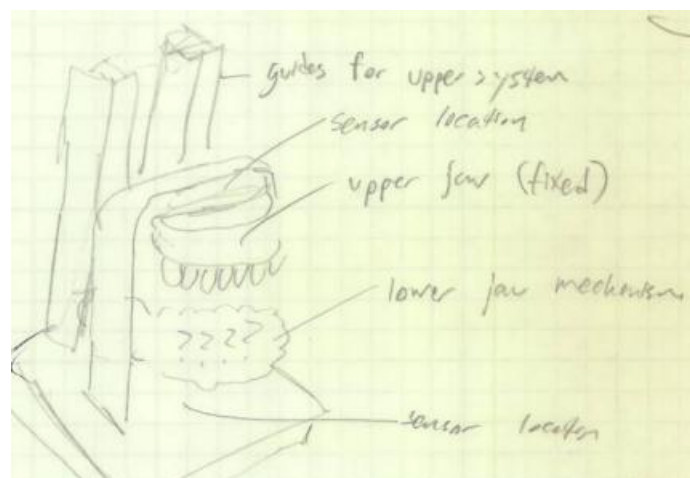


Figure 11. Mounting of maxilla.

With the mandible in motion, the maxilla must realistically be fixed to ground. An arch is added over the maxilla (Figure 11), which is connected to a base plate fixed to the stationary part of the Instron. Sensors will be added somewhere between the base plate and the maxilla for the measurement of reaction forces. This leaves the moving crosshead (translating vertically) and stationary base plate as attachment points for the mechanism moving the mandible.

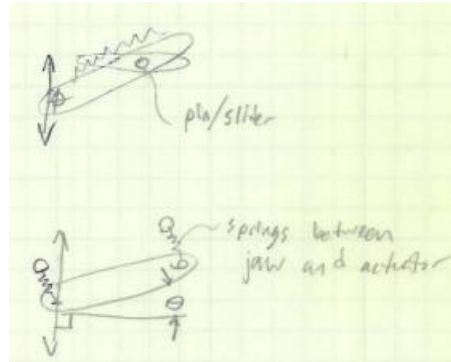


Figure 12. 1 DOF systems.

First considered were single degree of freedom systems (Figure 12). Simple pivoting is inadequate to model the jaw's motion. The design shown in the figure uses a pin-in-slot arrangement combined with vertical translation which allows for more complex motion, though it does not achieve a different return path, as is the case in actual mandibular motion.

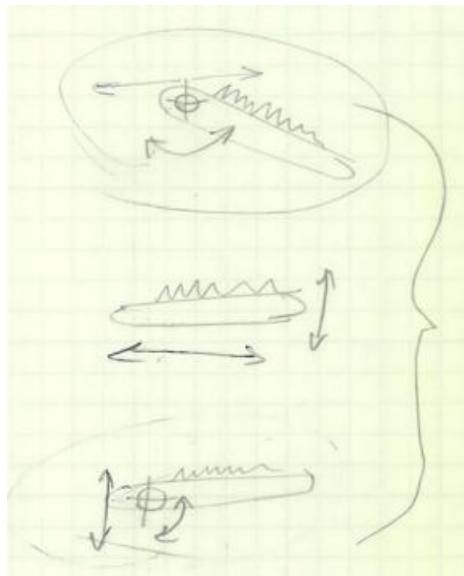


Figure 13. 2 DOF systems.

Adding a second degree of freedom expands possible motion of the fixture to the entire Sagittal plane. In Figure 13, this could result in either single-axis translation with rotation (top and bottom), dual axis translation (center), or all three modes. The top option, horizontal translation with rotation, most closely represents mandibular motion on the Sagittal plane, so this set of constraints will be seen as the most ideal when evaluating designs.

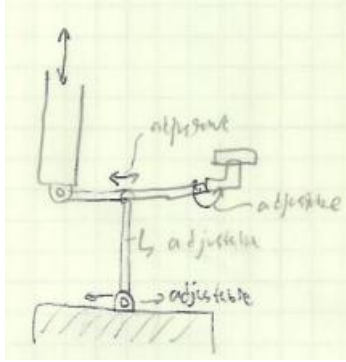


Figure 14. Pivoting linkage design.

Several early designs used linkages which use the difference in crosshead and ground velocities to simulate mandibular motion. The concept shown in Figure 14 allows for complex, adjustable motion, but runs into safety issues if the test is not stopped after it is over, as the mandible is forced through the maxilla.

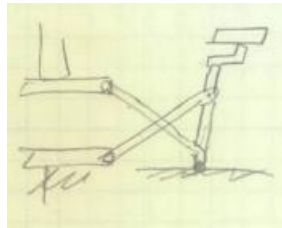


Figure 15. Crossed linkage design.

The concept shown in Figure 15 averts the collision issue, but does not model realistic motion. A number of other linkage designs were rejected for safety or realism issues. Additionally, iteration of nontraditional linkage designs such as these is heavily based on trial and error, and only offers a single motion profile once built (at this point in development, the possibility of multiple design profiles was still being considered). The design process would soon switch focus to more precise and controllable concepts.

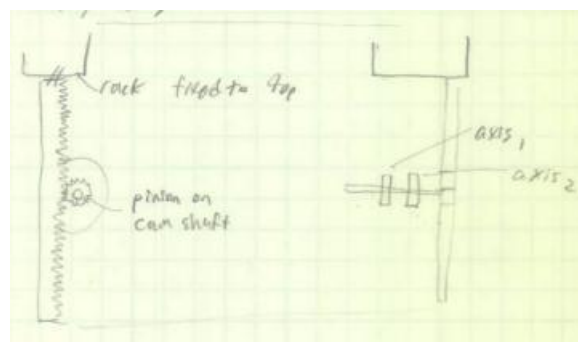


Figure 16. Pinion-driven rotary cams.

Cams offer a more controllable input-output relationship and therefore were the next machine element considered for concepts. If multiple motion profiles are desired, switching to another is as simple as switching the cams. First, the linear motion of the crosshead must be converted to linear

motion of cam followers. The first concept considered for cams (Figure 16) uses a rack on the crosshead to spin a pinion mounted to a pair of rotary cams. This allows the fixture to run multiple mastication cycles in a single test.

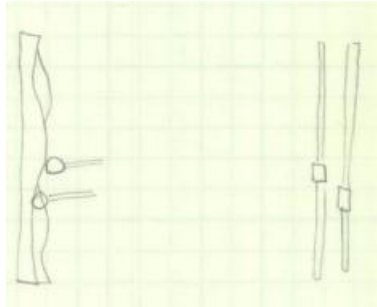


Figure 17. Linear cams.

Another concept uses a pair of linear cams (Figure 17). This eliminates the extra step of converting translational motion to rotational and back, which was expected to save some of the limited space at the base of the Instron. The advantage of being able to run multiple mastication cycles with rotary cams was judged to be smaller than the advantage gained by the extra space, so the concepts that follow will be based on linear cams.

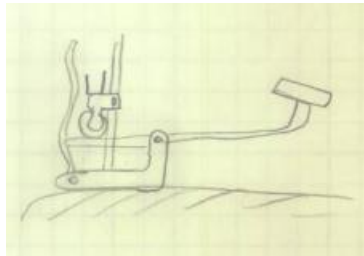


Figure 18. A cam-linkage system.

A cam-linkage system (Figure 18) uses once linear cam surface to control horizontal translation of the mandible, and a second hinge for rotation, moving the lever arm of the mandible with a roller. While this represents the 2 DOF model of the mandible directly, synthesis of the cam surface is difficult as the vertical position of the roller on the mandible's lever arm is dependent on the mandible's horizontal position, putting the two cam profiles out of sync and making the cam design especially difficult.

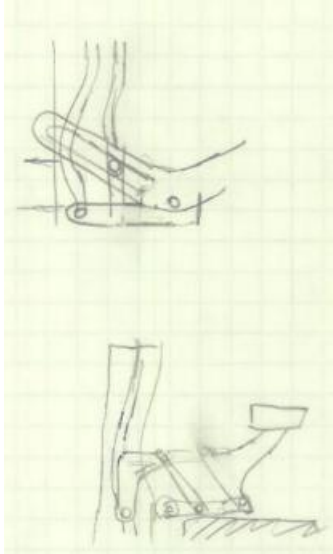


Figure 19. Another cam-linkage system.

The concept in Figure 19 attempts another direct relation between two cam profiles and translation/rotation, but faces the same cam synchronization problems as the previous design.

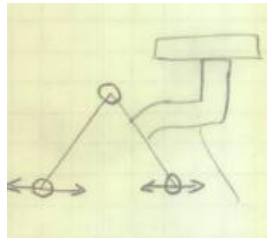


Figure 20. Double translating linkages.

A linkage concept, of which one linkage is attached to the mandible (Figure 20) allows for complex motion and solves the transient synthesis problem. When both links translate with a common velocity, the mandible translates horizontally. When the links translate with different velocities, the mandible moves with a combined translation/rotation.

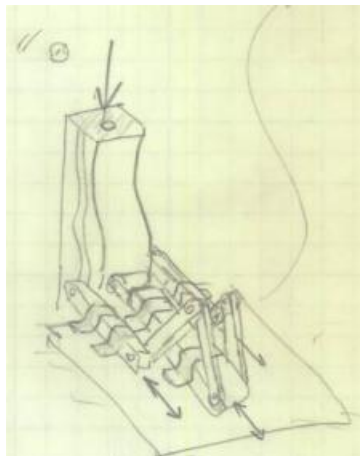


Figure 21. Symmetrical double-translating linkages.

Figure 21 shows the double translating linkages attached to a cam block with two different cam profiles. It was assumed that symmetry would improve structural integrity and repeatability between tests, but this was removed in the final design to allow both cam profiles to be machined into the sides of the cam block rather than on an exposed edge. Synthesis of the cam profiles would take place during the detailed design phase.

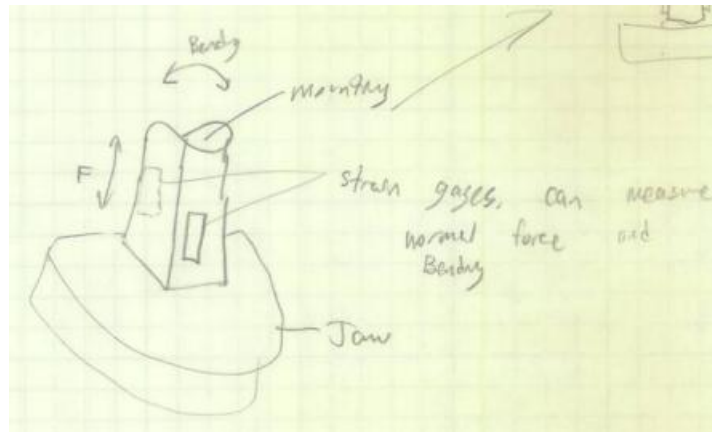


Figure 22. Early strain gage mounting concept.

With the motion of the cam accounted for, the next task was the mounting of sensors for measuring reaction forces on the sample. Strain gages were determined to be the most cost effective method. The concept in Figure 22 shows two strain gages mounted to the anterior and posterior faces of a support attached above the maxilla. Normal and shear forces would be calculated based on the magnitude and difference in the strain on each gage, respectively. This method was expected to have problems with accuracy in distinguishing between both kinds of forces.

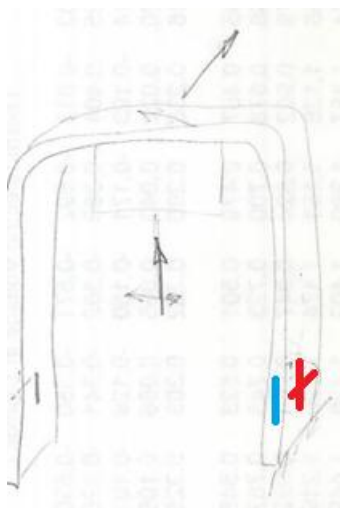


Figure 23. Support mounted strain gages (blue: shear; red: normal).

Additional research into industry use of strain gages led to better use of them in the fixture. Mounting separate sets of strain gages to the arch around the maxilla reduced the size of the mechanism and allowed for better discrimination between normal and shear forces (Figure 23, gages

are shown in blue). One gage each on the anterior and posterior surfaces of one support measure bending due to shear forces on that beam. These gages are mounted in a half Wheatstone bridge configuration. Since they are mounted at the base of the beam, these gages experience a significant mechanical advantage in bending which improves the resolution of their data.

Two gages are mounted at right angles to each other on the sides of one supporting beam (Figure 23, gages are shown in red) to measure normal force. On the sides, bending due to shear is absent entirely, though without any mechanical advantage this axis uses a full bridge to improve the resolution of the data.

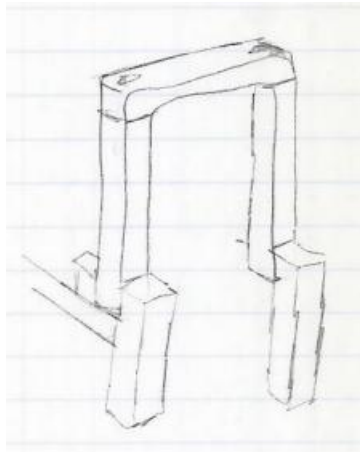


Figure 24. Fixing supports of the base.

The mounting of the supports of the maxilla to the base plate must approximate a fixed support joint as closely as possible so that a majority of the energy from the reaction force at the maxilla is applied to deforming its supporting beams and is measured by the strain gages. A concept shown in Figure 24 encloses the base of the supports on three sides for this purpose.

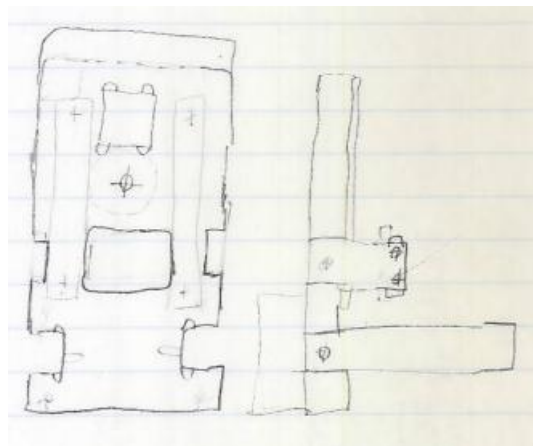


Figure 25. Base plate.

The base plate (Figure 25) was designed to better constrain the maxilla's supporting beams. Tolerancing in the final design provided a tight press fit for these supports



Figure 26. Modeled cam and cam mounting.

The cam and fixture body are shown in Figures 26 and 27, respectively. The model produced in Pro/Engineer is based on the double translating linkage concept. Details of the denture mounts (yellow, Figure 27) were left manufacturing due to the irregular and organic geometry, though the overall size of these parts was modeled in CAD. Effort was made to minimize the quantity of hardware types and stock material thicknesses. Careful tolerancing was provided on the linear bearings (light orange and sage) to allow smooth motion of the cam followers. .50" Aluminum was calculated to be adequate in all parts for bite forces up to 1000N, though it is expected that the dentures will fail before this point.

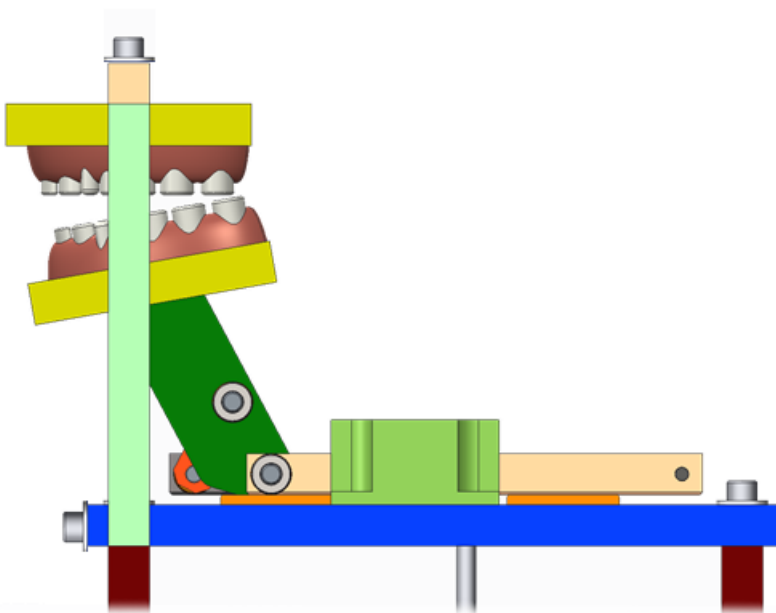


Figure 27. Modeled linkages, base plate, supports, and jaws.

Detail design involved little iteration other than the size of components related to cam profile synthesis (including linkages, forest green and orange, cam followers, gray and peach, and the length of the base plate, dark blue Figure 27). Dimensions of these parts were modified as required to accommodate cam synthesis. Data for a chosen motion profile was imported into Pro/Engineer and

projected over the mandible on the sagittal plane. To relate positions on the motion profile to positions on the cam, interactions between moving parts were defined in the mechanisms module of Pro/Engineer. The mandibular incisor tip was manually moved to seven points around a chosen motion profile (Table 3), and corresponding positions of the cam followers were marked at intervals on the surface of the cam. A best-fit spline was run through these points to define the cam profile (Figure 26). The surface of the cam profile was analyzed for acceptable pressure angles and velocities. Acceleration and jerk analysis were neglected due to the exceptionally slow speed of the crosshead, which does not exceed 100mm per minute in tests using this fixture.

Table 3. Positions of the cam over time.

point on profile	time (s) at 10mm/min	time (s) at 100mm/min	cam displacement (cm)	Phase of mastication
1	32.22	3.222	0.537	Compression
2	120.42	12.042	2.007	Compression
3	201.54	20.154	3.359	Compression
4	286.14	28.614	4.769	Compression-Shear Transition
5	370.86	37.086	6.181	Shear Region
6	455.46	45.546	7.591	Shear-Release Transition
7	540.18	54.018	9.003	Release
8	624.78	62.478	10.413	Release
9	709.5	70.95	11.825	Release-Compression transition

Since both halves of the dentures have a wedge-like cross section, both are mounted to aluminum bases using counter-facing wedges (see Figure 28 for a view of one counter-facing wedge on the mandible). Both the wedges and the alignment structures at the base of the denture mounting blocks are padded with silicone to prevent abrasion or fracture of the dentures.

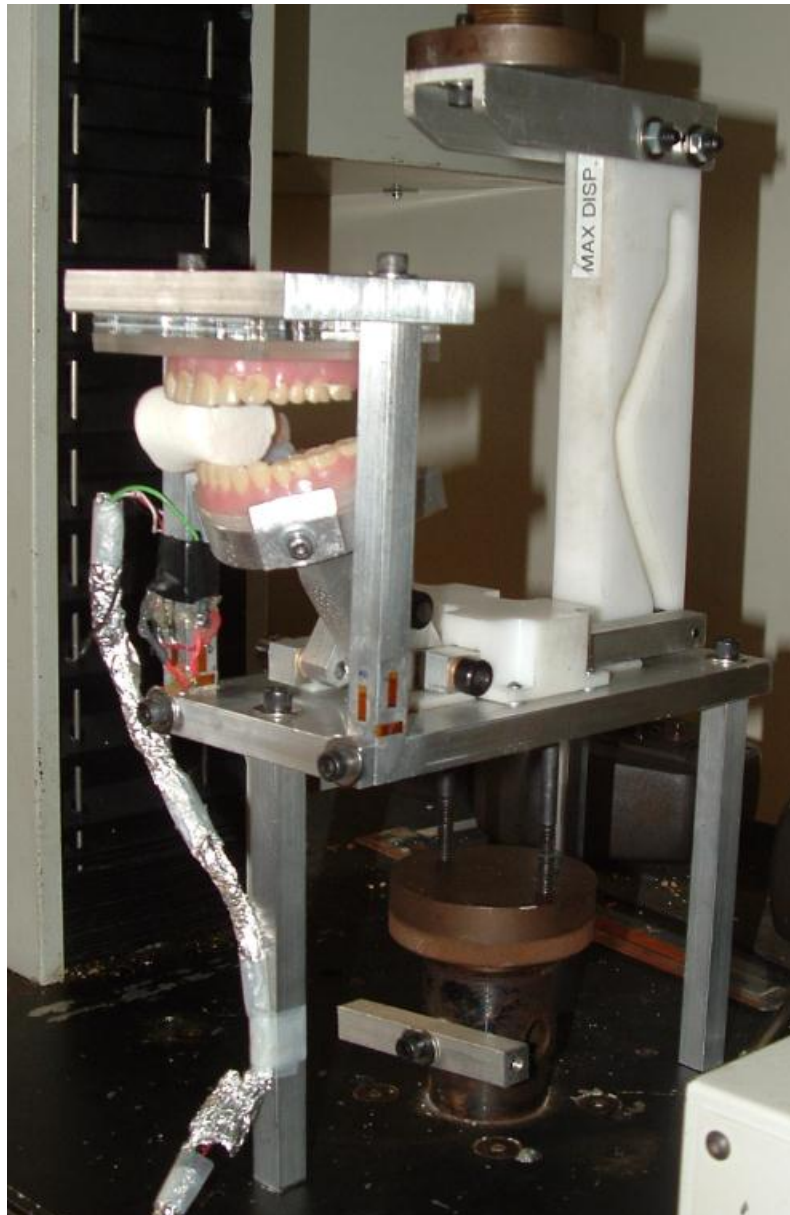


Figure 28. Manufactured fixture in Instron.

The manufactured fixture (Figure 28) has few differences from the CAD model. The linear bearings in the original design were separate for each cam follower, but alignment problems led to these being remade as a single piece. The mounting components for the maxilla and mandible came out larger than originally planned. As a result, the mandible's supporting linkage was shortened and the maxilla received longer supports.

As the Instron 4201 is capable of exerting large forces, several safety features are included in the design. The primary concern is that the cam block will collide with either the key supporting the base of the fixture or with the base of the Instron itself, and the resulting fracture would project shrapnel at the user. To address this concern, a custom key was manufactured which cannot be inserted in a way that interferes with the cam block. The cam profile also has a 'safety zone' after the mastication cycle that

gives the user additional time to stop the Instron after a test. Additionally, the fixture has markings which encourage its proper setup and use. The mastication fixture should only be operated by individuals who are familiar with its setup and use, who are wearing safety glasses, and are able to give the machine their full attention while testing.

5.0 Methodology

5.1 Fixture Calibration

The fixture is calibrated to accurately reflect the applied force relative to the measured voltage. A linear model is assumed for this procedure such that the force is directly proportional to voltage. Bending (shear) force is calibrated with the fixture laid down and a 1 kilogram mass suspended from the maxillary plate, applying the force in a single, positive direction (parallel to the sagittal/transverse planes). The measured voltage along this axis and in this direction then corresponds to 9.81 N. A similar procedure is used to calibrate normal force by placing a 1 kilogram weight on top of the maxillary plate and correlating the measured voltage with the 9.81 N applied force. This force is applied along the axis at the intersection of the sagittal and coronal planes.

5.2 Sample Preparation

Samples are prepared for testing by a standard method that allows for comparison between similar foods. All samples are prepared under standard atmospheric conditions and at room temperature, and maintained in this environment for the duration of testing. The weight of every sample is recorded prior to testing in order to indicate consistent sizing. Commercial products such as crackers or cereal pieces are used as whole pieces and are assumed to be standardized by the manufacturing process.

Produce and larger commercial foods (ex. apples and chocolate squares) require further preparation and standardization to produce consistent results. For situations when produce is used, fresh, medium-sized products without visually perceptible abnormalities are selected. Samples are cut with a sharp, clean knife from the interior without any part of the skin to eliminate surface effects. For samples that produce noticeable oxidative effects (i.e. apples and chocolate) samples are prepared within 10 minutes of testing.

5.3 Sample Testing

All sample testing takes place under standard atmospheric conditions and at room temperature. The cam is reset to a standardized position, where the bottom is flush with the underside of the fixture base plate. This allows for the full range of the mastication cycle with some delay time (dependent on sample dimensions) before the teeth contact the food. Samples are positioned with one edge aligned with the back of the right, third molar (tooth number 32), extending toward tooth #28 in the case of oblong samples. Dark chocolate samples (Lindt 70%, 90%; Ghirardelli 72%, 100%) are tested at an Instron crosshead speed of 100 mm/min and all other samples are tested at 10 mm/min. For dark chocolate samples, force-time data is also collected by the Instron machine by a load cell in the crosshead. Testing continues until complete jaw separation and the measured force returns to zero.

5.4 Data Analysis

A standardized analysis method is applied to the raw data output by the system. Force and time as recorded by the apparatus begins at a specific point in the masticatory cycle of the fixture which does not necessarily correspond with the time force is initially applied to the sample. Consequently, excess

data is trimmed from the beginning and end of each test and the first datum is designated the zero point at which elapsed time is defined to be zero.

The force data is also calibrated to a zero point by a standard method. The force observed before the zero point is assumed to be zero, although it is usually offset by some amount. Excluding aberrant data (transient electrical noise, manual force application), the force before the zero point is averaged (average force offset) and subtracted from the raw data. The net effect of this procedure is to shift the force-time curve either upwards or downwards and account for anomalous error that occurs between tests.

6.0 Journal Paper, Design of a Fixture for the Dynamic Evaluation of Forces During Mastication

The content that follows in this section was produced for submission to a prestigious academic journal, and covers the details of the design process for the mastication fixture.

Abstract

This paper describes the design process of a 2 DOF mastication fixture, an engineering model which allows for the measurement of forces in human mastication over the course of a mastication cycle. The design incorporates cam-driven sagittal motion of the mandible to allow multi-axis force measurements on a variety of food samples. The resulting fixture provides consistent data for brittle and lightly viscoelastic foods.

1 Introduction

The detailed measurement of bite force, or the force exerted by the jaw onto a food sample during mastication, is of interest to dentistry and both food engineering and quality control. The forces required to chew food can, from a materials standpoint, characterize the texture of a food as perceived by a human.

The most realistic environment to observe human mastication is the human mouth. While *in vivo* testing may be mandatory depending on what parameters are being tested, a simulated environment provides more consistent results without the obstructions created by buccal and lingual surfaces [1].

This problem is averted through the use of mastication simulators [2]. These devices simulate the conditions of the human mouth through mechanical, chemical, and/or thermal means [3]. Simulators which only take mechanical conditions into account still have advantages over conventional shear and compression testing in that the motion of the device and geometry of the surfaces in contact with the sample are nearly identical to *in vivo* testing [4].

Several of these simulators have been designed and built previously for the simulation of the human jaw's motion, such as Takanbu et al. [5], Villamil [6], and Conserva [7]. While other mastication simulators may seek to simulate the biological means of mastication (including modeling of muscle tissue in Takanobu et al. [8], and Takanishi et al. [9]), mastication simulators built for analyzing the textural properties of foods need only focus on realism as far as interactions with the sample are concerned.

2 Simulated Mastication

The mastication fixture presented in this paper is designed to measure the textural properties of food samples through the replication of the kinematics and geometry of occlusal surfaces in human mastication. While there are existing devices that provide this functionality (such as Salles et al. [10]), this fixture narrows the scope in terms of complexity of motion and experimental data to ease the analysis of the samples' textural properties. Additionally, this fixture is cheaper and easier to produce than contemporary mastication simulators.

2.1 Motion Profiles

The limits of the mandible's motion are defined by the kinds of motion allowed by the jaw as a whole. Mandibular movement on the sagittal plane consists of two modes, rotation and transverse translation, which relate to clenching (normal force) and grinding (shear force) respectively when in contact with food. Muscular and skeletal constraints put a boundary on the ranges of these motions. This boundary is known as Posselt's Sagittal Envelope, and all sagittal motion of the mandible must take place within its limits [11]. The overall size of the envelope can vary between individuals, though specific points are still analogous.

Movement of the mandible is typically measured with a trace curve at the tip of an incisor [12]. While the exact path followed by the human jaw varies with several factors including the kind of food being chewed and the age and gender of the person chewing, these paths are composed of variations of two primary movements: clenching and grinding [13]. *Clenching* refers to the closing of one's jaw with no translation. *Grinding* involves mastication with translation such that teeth slide across each other while chewing.

2.2 Simplified Motion Profile

Other studies such as Daumas et al. have mapped motion profiles for a variety of individuals and types of food [14]. For the purposes of standardization of results in this paper, it is desirable to define a single motion profile that is representative of several chewing styles. This will allow for a simpler mechanism and a broader characterization of textural properties.

While more complex motion of the jaw is useful in mastication robots built to analyze forces within the mouth, the Fixture presented in this paper uses a *simplified motion profile*, which is composed of a path which still incorporates both clenching and grinding, which results in the motion profile shown in Figure 1, which is within Posselt's Sagittal Envelope for an individual of average size. Since the fixture's purpose is the characterization of foods' texture rather than analysis of forces within the mouth, this simplification eases the analysis of the food samples' material properties while maintaining realistic mastication kinematics.

3 Masticatory Fixture

Testing of food samples using the kinematics defined in the previous section requires a mechanism that is able to consistently provide this mandibular motion and collect relevant force data. While the actual motion of the human jaw can involve translation and rotation on the sagittal and coronal planes, a simplified model of translation and rotation on the sagittal plane alone still allows for the collection of data for both Shear (F_S) and Normal (F_N) forces on the foods under test. The overall fixture model includes the mechanism, a compression/tension testing machine for actuation and chronometric consistency, a sensory system for measuring forces, and a computer for storing sensory data.

3.1 Mechanism

The mechanism portion of the fixture consists of a set of cams and linkages which are driven together to produce the simplified motion profile at the tip of the mandibular incisor. The experimental setup of the mechanism can be seen in Figure 2.

Linkages

The linkage supporting the mandible (Figure 2) is manipulated by two sliding linkages which are themselves attached to two cam followers. Movement of the sliding linkages at a common direction and velocity allows for translation normal to the coronal plane, whereas motion of the sliding linkages with different velocities allows for a combined translation/rotation on the sagittal plane. The range of positions allowed by these two kinds of motion allows the tip of the mandibular incisor to be moved to any point on the simplified motion profile.

Cam

The cam block (Figure 2) features two cam profiles, one on each side of the block, which together produce the simplified motion profile of the mandible. To create the cams' shapes, the mandible was moved to points along the simplified motion profile in a CAD package, and the resulting positions of the cam followers were plotted on the surfaces of the cam block. The dimensions of the linkages and the cam block were iterated to allow for safe pressure angles and mandibular velocities that allowed for more data collection. In particular, this meant that the portion of the experiment between the end of clenching and the beginning of release would move more slowly as this was the region in which samples were expected to fracture. Since the cam block is driven by the constant velocity crosshead of the Instron 4201, the position of the mandible with respect to time is consistent between tests of different food samples.

The table shown in Figure 3 relates the displacement of the cam to key regions on the simplified motion profile and the passage of time in the experiment. This is useful for relating features in the experimental data to details of the mandible's motion directly.

Occlusal Surfaces

As the geometry and material of surfaces in contact with the food sample can have a significant effect on the measured forces and the nature of the fracture of the sample, it is important to provide a realistic representation of occlusal surfaces. In this fixture, the mandible and maxilla used the corresponding halves of a set of dentures for this purpose. These halves are mounted to the frame and linkages of the fixture using silicone-padded aluminum and acrylic fittings. A light layer of silicone is also added to the base of the dentures to simulate the softness of the gingiva.

3.2 Data Collection

The data collection portion of the fixture consists of the strain gages, the amplification of their signal, and their storage on the hard disk of a computer.

Sensory System

Since it is impractical to measure strain on the food samples directly, the fixture incorporates strain gages attached to the maxillary supports. The sensors' measurements for strain due to tension and bending on the supporting beam (attached to wires, Figure 4) are converted to F_N and F_S , respectively, as reaction forces on the sample. F_N measurement features four strain gages in a full Wheatstone bridge configuration to improve resolution and temperature compensation. Since F_S is measured as strain due to bending at the

base of the beam, it assumes a relatively high mechanical advantage and therefore a high level of strain compared to the actual force at the maxilla.

Amplification and Computer Interface

Strain gage data from the F_N and F_S channels is cleaned and amplified through two Vishay 2310 strain gage amplifiers, and sent through a National Instruments NI USB-6008 for interface with LabVIEW. Stored data includes elapsed time, raw strain gage data, calculated forces, and sample rate. These data are exported for analysis in other programs as defined in a paper by Spangenberg [15].

Calculated forces are based on calibration performed before the start of a test, in which weights representing known forces are attached to appropriate parts of the maxilla. Normal force is calibrated by placing a weight on the top surface of the frame supporting the maxilla, centered about the sagittal plane. Shear force is calibrated with the frame tilted forward 90 degrees and a weight suspended at the level of the maxilla's occlusal surface.

Each axis is calibrated to $\frac{1}{2}$ of the applied weight as the strain gages are only mounted to one of the two supports. Accuracy of the calibration was confirmed with several different weights.

4 Experiment

Once the fixture is loaded into the Instron as shown in Figure 4 and a food sample is inserted between the jaws, a single test consists of running the fixture from a starting position marked on the cam block until there is no observable contact between the food sample and the surfaces of the teeth (which is confirmed by a near zero force reading on the LabVIEW Virtual Instrument).

4.1 Food Sample Data

While this paper focuses on the development of the mastication fixture, a basic analysis of the data it is able to produce is useful in determining the fixture's overall effectiveness in analyzing the texture of food samples.

Effort was made to consistently align samples at the same position between the jaws. One edge of the sample was aligned with the rear edge of tooth 32, and positioned laterally to avoid sliding during the test and to avoid interference with the maxilla's supporting columns. However, there are small variances between tests due to small differences in positioning and the geometry of the food under test.

An example of the recorded data is presented as graphs of F_N and F_S with respect to time, which can be correlated with respect to the simplified motion profile with Figure 3. Data averaged between tests does not show the characteristics of the test accurately due to the variations described in the previous paragraph, especially for tests of brittle food samples. For this reason, the graphs shown in this section are created with representative rather than averaged tests.

Brittle Samples

Tests using brittle foods are characterized by many smaller fractures over the course of the compression and shear regions of the mastication cycle (see Figures 5 and 6). During a test, it is observable that points

on the molars and premolars (and even canines and incisors for longer samples such as club crackers) induce 3-point bending on local sections of the sample.

Highly Viscoelastic Samples

Foods with a high level of viscoelasticity cannot be accurately tested on the mastication fixture, especially when the Instron is set to run at lower speeds. Foods such as marshmallows and a variety of cheeses tested in the fixture rarely experience forces more than an order of magnitude greater than noise present in the signal (Typically $\sim 2\text{N}$ on the F_N plot). Vermont Sharp Cheddar cheese is fairly representative of this phenomenon and can be seen in Figure 7, with some observable shape but a large signal to noise ratio. In such tests, the sample deforms so slowly that it is able to ‘flow’ out of the gap between both sets of molars. With no apparent fracture in the recorded data, the sample was often removable after the tests as a single piece of material, albeit deformed from its original state.

The author expects that a higher strain rate will lead to better data acquisition for highly viscoelastic materials. Additionally, a reduction in signal noise will improve the usefulness of data collected from very soft foods such as cheeses, breads, and marshmallows. Many of these materials may be qualitatively observed to exert adhesion during the release phase, though between noise and some slop in the mechanism this event is unobservable in the data.

Lightly Viscoelastic Samples

While materials with high viscoelasticity do not test well with the mastication fixture, harder, less viscoelastic samples display both a more consistent force plot over the course of a mastication cycle than brittle foods and large enough forces to stand out against the noise in the system.

Tests with these kinds of samples focused on commercial chocolates with varying amounts of cacao, to test if the fixture was sensitive to more subtle differences in food samples such as cacao content. With other factors the same, it was expected that chocolate’s fracture toughness would increase with cacao content. Two types of Lindt (70% and 90%) and two types of Ghirardelli (72% and 100%) chocolate were tested, and F_N and F_S data from these tests were simplified to a resultant force by

$$F = \sqrt{F_N^2 + F_S^2}. \quad (1)$$

The resultant force was then plotted for the four samples as seen in Figure 8.

It can be seen in Figure 8 that the magnitudes of the peak resultant force measured for each sample follows the same order as the cacao content, as well as an increasing brittleness. The area under each curve, which is approximately proportional to fracture toughness, follows a similar order, with some variation due to the fact that Lindt chocolates of different cacao content have different hardness (measured separately) even when cacao content is not taken into account. This relationship was confirmed with basic compression testing on the Instron.

A more detailed analysis of the textural properties of chocolate through the use of this fixture can be found in Spangenberg’s “Dynamic Evaluation of Texture in Chocolate” [15].

5 Conclusions

- 1) The fixture can measure textural qualities in foods and distinguish between incremental variations of a single ingredient's effect on toughness and brittle fracture.
- 2) The fixture can accurately measure reaction forces applied to brittle and lightly viscoelastic foods.
- 3) Improvements to the strain rate and the resolution of the sensory system will improve experimental data for all kinds of samples.

Acknowledgement

This project was completed with the help of several individuals who offered professional advice and technical guidance. The design of this fixture is part of a larger project in which Anthony Spangenberg has done an equal share, and much of the testing and analysis is a result of his labor. Additionally, I would like to thank Prof. Satya Shivkumar for his extensive knowledge of materials, food engineering, and academic documentation, and Prof. John Hall, Prof. Robert Norton, Fred Hutson, Randy Robinson, Neil Whitehouse, Toby Bergstrom, Adam Shears, and Maximilian Kaiser for their support in the production of the fixture.

REFERENCES

- [1] Kawashima, K., Miura, H., Kato, H., Yoshida, K., & Tanaka, Y. (2009). The study of comminution behavior of food on buccal and lingual side during mastication. *Journal of Medical Dental Science*, 131-8.
- [2] Conserva, E., Menini, M., Tealdo, T., Bevilacqua, M., Pera, F., Ravera, G., et al. (2008). Robotic Chewing Simulator for Dental Materials Testing on a Sensor-Equipped Implant Setup. *International Journal of Prosthodontics*, 501-508.
- [3] Salles, C., Tarrega, A., Mielle, P., Maratray, J., Gorria, P., Liaboeuf, J., et al. (2007). Development of a chewing simulator for food breakdown and the analysis of in vitro flavor compound release in a mouth environment. *Journal of Food Engineering*, 189-198.
- [4] (2011). Retrieved March 9, 2012, from Texture Technologies: <http://www.texturetechnologies.com/texture-analysis/Probes-Fixtures.php>
- [5] Takanbu, H., Takanishi, A., & Kato, I. (1993). Design of a mastication robot mechanism using a human skull model. *Intelligent Robots and Systems*, 203-208.
- [6] Villamil, M. B., Nedel, L. P., Freitas, C. M., & Maciel, A. (2005). A Model to Simulate the Mastication Motion at the Temporomandibular Joint. San Diego: International Society for Optical Engineering.
- [7] Conserva, E., Menini, M., Tealdo, T., Bevilacqua, M., Ravera, G., Pera, F., et al. (2009). The Use of a Masticatory Robot to Analyze the Shock Absorption Capacity of Different Restorative Materials for Prosthetic Implants: A Preliminary Report. *International Journal of Prosthodontics*, 53-55.
- [8] Takanobu, H., Yajima, T., & Takanishi, A. (1997). Development of a Mastication Robot Using Nonlinear Viscoelastic Mechanism. *IEEE International Conference on Intelligent Robots and Systems*, 3, 1527-1532.
- [9] Takanishi, A., Tanase, T., Kumei, M., & Kato, Ichiro (1991). Development of a 3 DOF jaw robot WJ-2 as a Human's Mastication Simulator. *IEEE Fifth International Conference on Advanced Robotics*, 1, 277-282.
- [10] Salles, C., Tarrega, A., Mielle, P., Maratray, J., Gorria, P., Liaboeuf, J., et al. (2007). Development of a chewing simulator for food breakdown and the analysis of in vitro flavor compound release in a mouth environment. *Journal of Food Engineering*, 189-198.
- [11] Wilson, P. H. R., & Banerjee, A. (2004). Recording the retruded contact position: a review of clinical techniques. *British Dental Journal*, 196, 395-402.
- [12] Peyron, M., Mioche, L., Renon, P., & Abouelkaram, S. (1996). Masticatory jaw movement recordings: A new method to investigate food texture. *Second Rose Marie Pangborn Memorial Snopsium*, 7, 229-237.
- [13] Takanobu, H., Yajima, T., Nakazawa, M., Takanishi, A., Ohtsuki, K., & Ohnishi, M. (1998). Quantification of masticatory efficiency with a mastication robot. *Robotics and Automation*, 1635-1640.
- [14] Daumas, B., Xu, W., & Bronlund, J. (2005). Jaw mechanism modeling and simulation. *Mechanism and Machine Theory*, 821-833.

[15] Spangenberg, A. (2012). *Dynamic Evaluation of Texture in Chocolate*. (Unpublished dissertation). Worcester Polytechnic Institute, Worcester, Massachusetts.

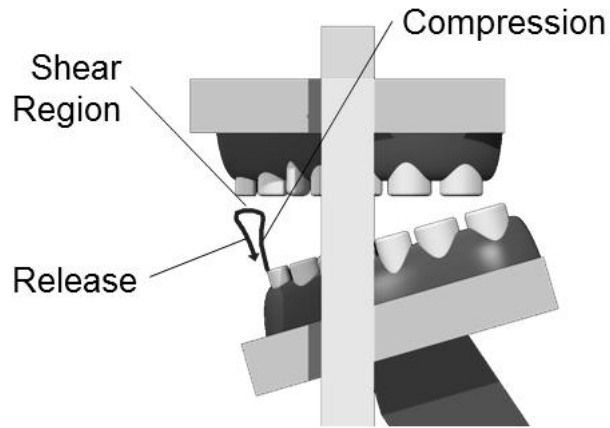


Figure 1. The simplified motion profile.

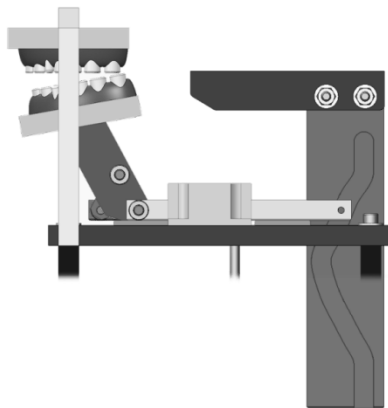


Figure 2. Mechanism.

point on profile	time (s) at 10mm/min	time (s) at 100mm/min	cam displacement (cm)	Phase of mastication relative to Figure 1
1	32.22	3.222	0.537	Compression
2	120.42	12.042	2.007	Compression
3	201.54	20.154	3.359	Compression
4	286.14	28.614	4.769	Compression-Shear Transition
5	370.86	37.086	6.181	Shear Region
6	455.46	45.546	7.591	Shear-Release Transition
7	540.18	54.018	9.003	Release
8	624.78	62.478	10.413	Release
9	709.5	70.95	11.825	Release-Compression transition

Figure 3. Mandibular motion relative to cam.

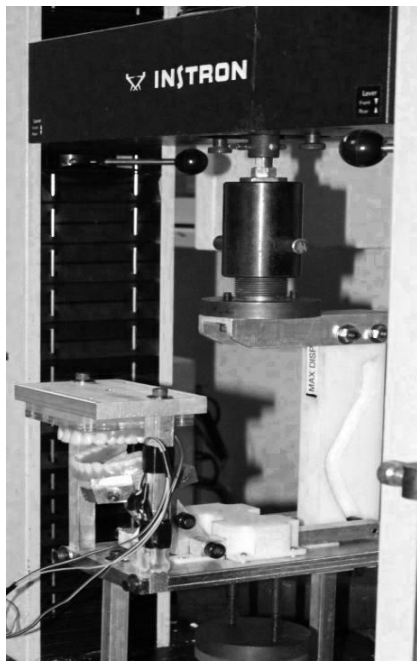


Figure 4. Mastication fixture installed.

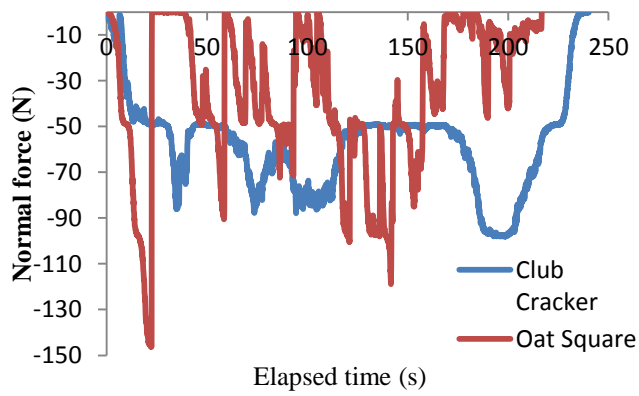


Figure 5. Brittle food normal force profile (10 mm/min)

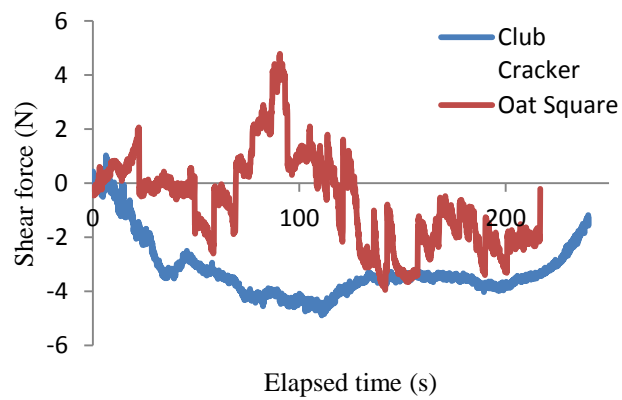


Figure 6. Brittle food shear force profile (10 mm/min)

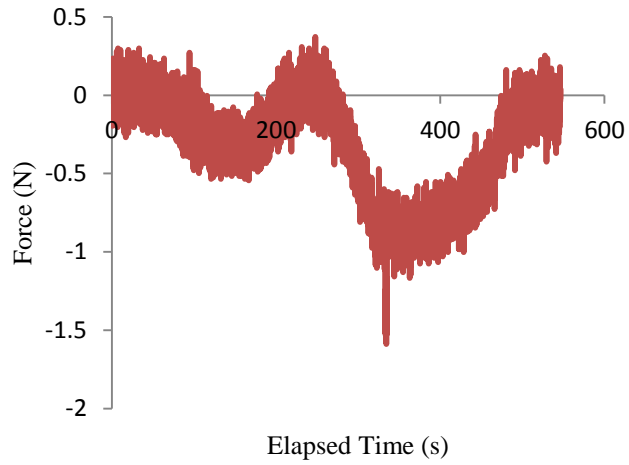


Figure 7. Vermont cheddar shear force profile (10 mm/min)

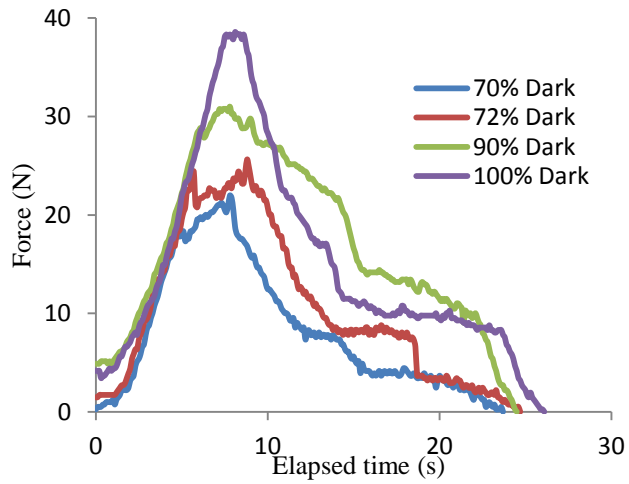


Figure 8. Chocolate resultant force profile (100 mm/min)

7.0 Journal Paper, Dynamic Evaluation of Texture in Chocolate

The content that follows in this section was produced for submission to the Journal of Texture Studies, and covers the details of the analysis of material properties in several different kinds of chocolate.

Abstract

Mechanical properties of foods are indicative of texture perception and product composition. By investigating parameters relevant to a food's texture profile it will be possible to predict reception by consumers and product quality. A novel means of interpreting food texture is explored using an imitative mastication simulator driven by an Instron testing machine to investigate properties of various types of chocolate. Statistical analysis is employed to detect predictors of intrinsic food characteristics and to discriminate chocolate types. A correlation is developed to predict cacao content of a chocolate based on measured hardness.

Practical Applications

Textural properties of foods are a primary factor in the consumer's evaluation of a product, and so have an influence on their decision to purchase it. Development of a pleasing food texture is therefore imperative for retaining a customer and maintaining a competitive product. The construction of a simplified simulator which is imitative of the mastication process will produce information indicative of the consumer's perception of a given comestible. Such a device will see applications in the food industry by giving food engineers texture profiles which yield insight into the reception of a new product without the use of excessively complicated machinery or sensory panels. By discrimination of similar foods, the device is also applicable in process quality control for the identification of aberrant products.

Introduction

Textural attributes of foods have been examined for their complex role in food perception for over half a century. (Kress-Rogers, et al., 2001) It is now well understood that texture as sensed by the human body is the product of a complicated interplay of measurable quantities. In order to interpret real-time changes in foods under an applied stress, various forms of the Texture Profile Analyzer (TPA) have been employed, beginning with the groundbreaking 1963 study by Szczesniak. (Szczesniak, et al., 1963) TPA uses descriptive parameters including hardness, cohesiveness, elasticity, adhesiveness, brittleness, chewiness, and gumminess based on measurements obtained from a plunger-like probe testing apparatus. In her work and other similar texture studies, the measurable quantities are used in correlational models that attempt to predict sensory parameters determined by human panels.

The most accurate data for measuring perceived textural parameters of foods would be obtained from *in vivo* measurements of a human subject chewing. However, limitations occur when interference from the measurement tool obscures data and creates a texture profile that is not truly descriptive of the food's texture. (Boyar, et al., 1986) Some experimenters have gone around this by taking EMG readings during mastication in order to correlate them with sensory evaluation, but without measurement of textural properties. Peng *et al.* showed a correlation between total energy of chewing and sensory hardness ($r=0.77$) and Sun *et al.* indicate a correlation of $r=0.95$ between the same variables. (Peng, et al., 2002 and Sun, et al., 2001) Therefore, imitative tests using mastication simulators have been developed in order to recreate the process so that sensors can be attached to measure food texture unobstructed. This is because forces as observed by a human can be recreated with a model having similar material properties to the human body and geometry/kinematics that match the mastication process. (Conserva, et al., 2008 and Meullenet, et al., 1997)

Well known imitative experiments include the series of papers by Szczesniak exploring the use of the General Foods Texturometer (1963) (Rosenthal, 1999), Bourne's work with the Instron testing machine (1968) (Bourne, 2002), and Meullenet's adaptation of TPA using a fixture with dentures (Meullenet, et al., 1997). Each experimenter utilized a two-cycle procedure in which the sample is deformed twice to the same extent. Meullenet later showed that it was possible to reduce the procedure to a single cycle while still extracting significant textural information. (Meullenet, 1999) His experiment showed strong correlations between measurement of hardness, fracturability, and cohesiveness with their sensory counterparts ($r=0.91, 0.92, 0.83$, respectively). A study on the texture of gelatin later showed that food hardness alone is a significant predictor of food texture experienced by human subjects. (Okiyama, et al., 2003) This was accomplished by using gels of different hardness and correlating the known differences in texture with the maximum occlusal force output by a human subject.

Mastication is considered to be a time-dependent procedure, where variables such as enzymatic action of saliva, applied strain rate, and sample viscosity affect the way texture is experienced. (Lucas, et al., 2004) At the start of mastication, the intention is to produce mechanical fracture of the food so as to increase surface area for subsequent stages of digestion. Time-dependency can therefore be eliminated by simplifying the procedure to a single cycle of testing at discrete strain rates, while still allowing extraction of sample hardness and fracturability. Because it is known that these parameters have a significant correlation with sensory data, this simplification will produce a reasonable approximation of the texture experienced by the consumer. It is then possible to minimize the procedure for texture profiling while still producing data which is comparable to similar studies at a reduced cost.

Materials and Methods

Force data measured by the fixture are reaction forces applied to the fixture by the samples. These forces are obtained by strain gages on multiple axes, yielding shear force (F_S) and normal force (F_N). Throughout analysis of the data, these are grouped together as a resultant force (F_R) according to:

$$F_R = \sqrt{F_S^2 + F_N^2}$$

which is the total force applied to the sample. Instron force-time data is also captured simultaneously. This information can be easily transformed to force-position data because of the constant velocity of the crosshead.

Chocolate samples are prepared for testing by a standardized procedure to allow for comparison between foods that are manufactured by dissimilar methods. Samples are stored, prepared, and tested at STP to eliminate oxidative effects which may alter the nature of the fat crystal structure. Chocolate pieces are cut with a clean, sharp knife to 1 cm x 3.7 cm pieces, and the thickness is the same across chocolate types. Samples are weighed prior to testing to ensure consistent sizing, and it is found that the ratio of standard deviation to average mass ranges from 2.17% to 6.33% between all samples tested.

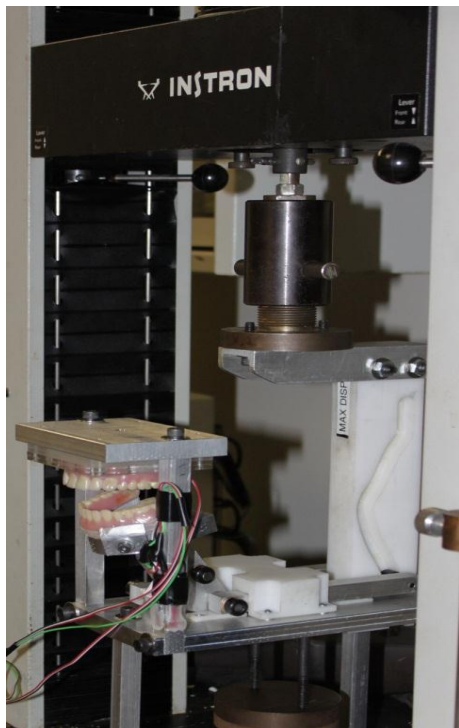


Figure 1. The imitative mastication simulator used for sample testing.

Testing is performed by zeroing the position of the fixture's cam to a location where it is flush with the underside of the fixture. From this position, an entire iteration of the mastication cycle can occur in addition to some delay time before the sample is contacted by the maxillary teeth. Samples are positioned with one edge flush with the back of the right, third molar (tooth number 32), extending toward tooth number 28 in the case of oblong samples. Samples are tested at an Instron crosshead speed of 100 mm/min. For dark chocolate samples, force-time data is also collected by the Instron machine by a load cell in the crosshead. Testing continues until all contacting teeth separate from the sample and the measured force returns to zero. More information regarding design and properties of the fixture can be found in McGarry's "Design of a Fixture for Dynamic Evaluation of Forces During Mastication." (McGarry, 2012) The fixture used is depicted in Figure 1.

Results

Representative data samples comparing each of the five chocolate types tested are given in Figure 2. The curves show both the characteristic texture of chocolate and how it varies according to cacao content. These curves indicate the distinction between similar chocolate types, where those with greater cacao content generally attain a greater hardness. It can also be seen that Ghirardelli chocolate is significantly harder than Lindt chocolate. Four primary features should be noted: 1) loading of the sample along the initial slope, 2) maximum hardness at the peak, 3) primary fracture of the sample where applied force drops dramatically (not present in milk chocolate), 4) compaction of the chocolate across the plateau region following fracture.

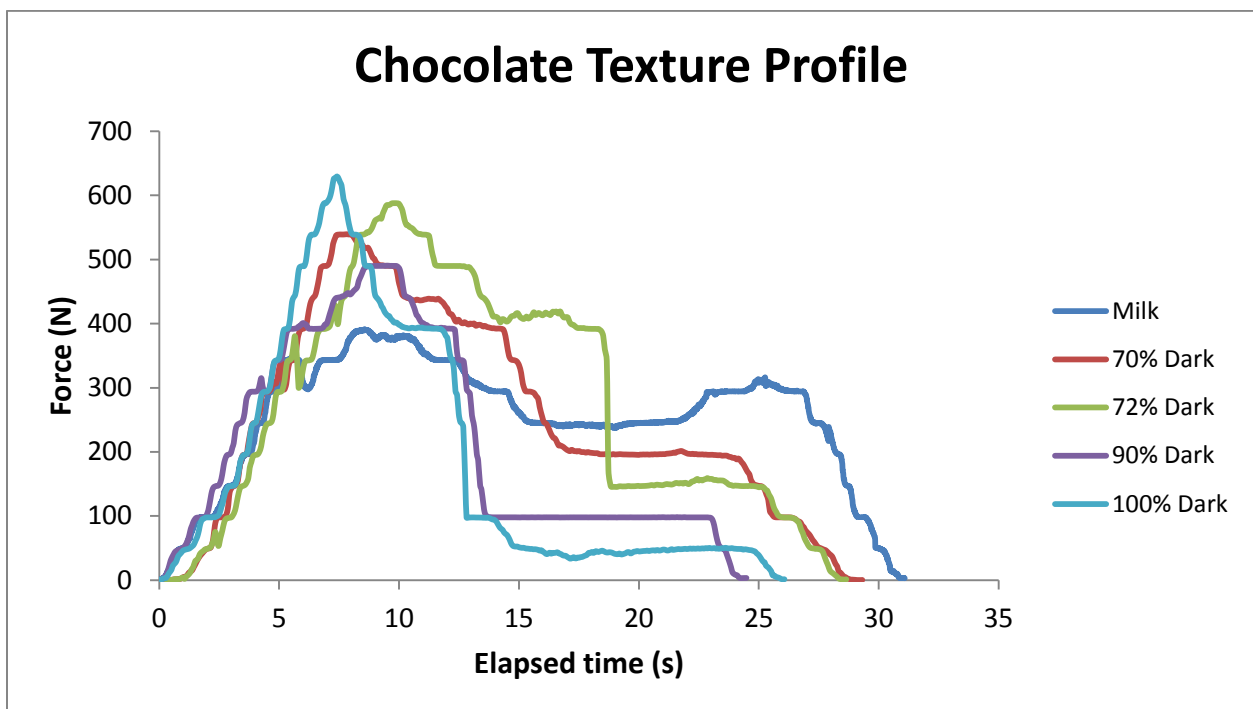


Figure 2. Representative texture profiles of each chocolate type tested.

Motion of the teeth is not at constant velocity or angular velocity despite constant input from the Instron machine. Therefore it is challenging to represent force as a function of position and evaluate the work expended in fracturing the food based on fixture data alone. By simultaneously recording data with the Instron, force can be determined as a function of position, from which work of fracture can be extracted. As an internal check of the fixture's validity, it should be expected that this work will correlate with the area under the curve between $t=0$ and fracture for data produced by the fixture (units of $N*s$). It was found that the correlation between the two has $r^2=0.9718$ for Lindt 70% dark chocolate. Chocolate types could

not be compared with each other because of friction between the fixture and Instron machine, which was not consistent each time the fixture was mounted. Based on this it can be seen that the integral to fracture of the fixture data is proportional to the work of fracture.

Average hardness for each chocolate type tested is plotted against percentage of cacao content in Figure 3. The figure indicates the expected result that increasing cacao content increases the measureable hardness of the food.

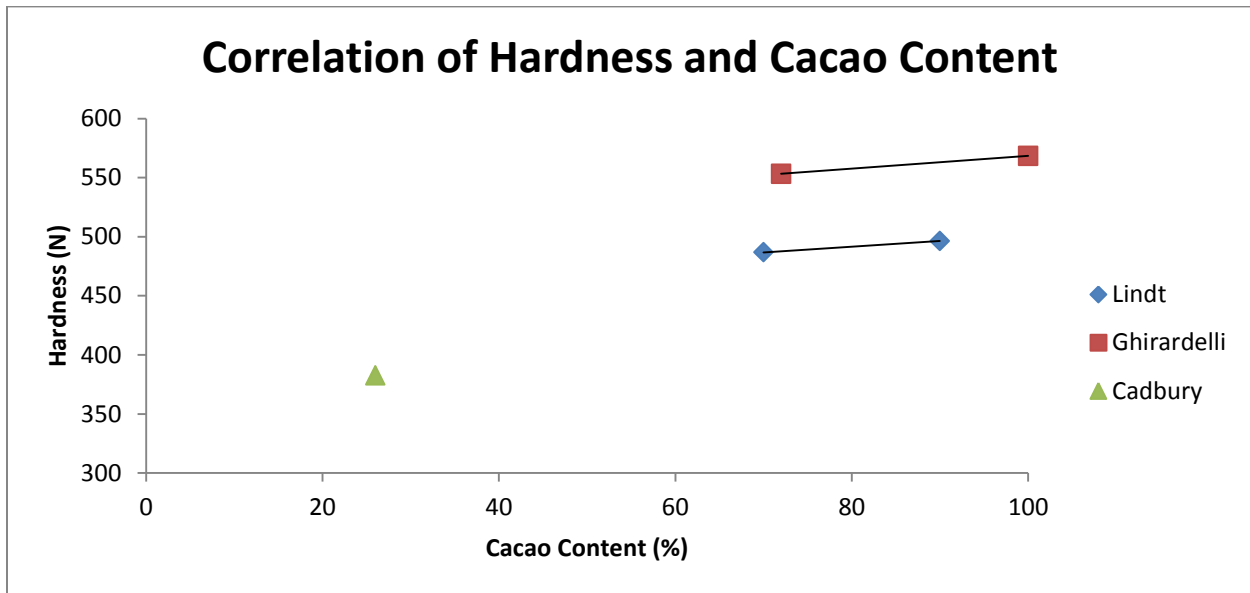


Figure 3. Influence of cacao content on chocolate hardness.

The equations describing Lindt and Ghirardelli chocolate hardness as a function of cacao content are:

$$\text{(Lindt)} \quad y = 0.4807x + 453.09$$

$$\text{(Ghirardelli)} \quad y = 0.5418x + 514.24$$

Data gathered for sample hardness and fracturability is displayed in Table 1, including sample standard deviation of each and the range across samples. Fracturability for milk chocolate is not included because it does not undergo brittle fracture during any test run.

Table 1. Average hardness and fracturability of samples by chocolate type.

Chocolate	Hardness (N)	Hardness Range (N)	Fracturability (N)	Fracturability Range (N)
Cadbury Milk 26%	382.44±45.44	108.6	N/A	N/A
Lindt 70%	486.7±45.96	112.2	292.5±1.614	3.870
Lindt 90%	496.4±10.16	23.50	305.0±23.94	48.77
Ghirardelli 72%	553.3±54.02	96.90	376.0±28.53	50.17
Ghirardelli 100%	568.4±86.91	186.4	404.7±21.07	37.20

In order to discriminate chocolate types, Student t-testing is applied. An unpaired, single tail, heteroscedastic test is used. Differentiation within chocolate types and between different makes is examined in Table 2.

Table 2. T-test values comparing makes of chocolate and effect of cacao content.

	Lindt 70 vs. Ghirardelli 72	Lindt 90 vs. Ghirardelli 100	Lindt 70 vs. Lindt 90	Ghirardelli 72 vs Ghirardelli 100
t-test value	0.120682	0.002475	0.295946	0.102519

Based on the t-test it can be seen that Lindt 70% and Lindt 90% chocolate cannot be differentiated from each other based on hardness alone. It should be expected that Lindt 90% and Ghirardelli 100% can be easily differentiated (different make and relatively different cacao content). This is verified by the t-test, where the calculated value is significantly less than any relevant p-value that could be selected for the test. T-test values comparing Lindt 70% with Ghirardelli 72% and Ghirardelli 72% with Ghirardelli 100% are just outside a p-value of 0.1, which suggests that differentiation between within the pair would be incorrect 10% of the time.

Discussion

The fixture enables the user to obtain a representative texture profile that gives insight into the nature of the test food. Various stages can be identified from the force-time texture profiles which are indicative of sample failure behavior. The data show the difference between the brittle and ductile failure modes of dark and milk chocolate, respectively. From texture profiles generated, hardness, fracturability, and work of fracture can be determined. It is also possible to determine other properties which may explain material behavior because a full texture profile is produced. Average hardness across a number of samples can allow differentiation between makes of chocolate tested, but not necessarily determination of cacao content. Based on the t-values found relating different makes of chocolate, it should be possible to differentiate these with improvements to the fixture.

Deviation in the measurements contributes significantly to the inability to distinguish cacao content from hardness. This error is largely a product of sample slippage while in contact

with the teeth. Although sample size is standardized in order to give consistency on a test-to-test basis, contact area with the teeth does not remain constant as the sample fractures and pieces dislodge. In order to counter this, it is recommended for future studies that buccal and lingual surfaces be added to constrain the sample and standardize contact area throughout the test procedure. Improvement in the sensitivity of the fixture will improve resolution of the data gathered and also allow for better distinction of chocolate types. An increment of 0.481 N/1% cacao was observed in Lindt chocolate. Relative to the 10.16 N standard deviation in Lindt chocolate (the smallest deviation observed), it is impossible to distinguish small changes in cacao content based on hardness alone.

Standard deviations and representative texture profiles would be further improved by increasing the number of samples tested for each chocolate type. Testing a larger variety of chocolate types will allow for better comparison between chocolate makes and support the correlation of hardness and cacao content. Testing a greater variety of foods will also yield characteristic curves for other food types and allow for better understanding of the fixture's performance. Additionally, hardness evaluation by a sensory panel will further validate the data. Correlation with sensory data will corroborate the differences observed between chocolate types and cacao content, and will also verify the accuracy of the fixture.

Overall the concept of using the fixture for product discrimination is feasible based on the results of this study, although future refinements must be made. Correlation with sensory panel data would help to corroborate the data generated by the fixture, and indicate that it is an accurate representation of human perception. This would validate the simplifications made and ensure that the method used is appropriate. It should be noted that the approach for this study is distinct from TPA and should not be directly compared with its method or results. The fixture described by this study is intended to provide the nature of food texture for the purpose of general comparison. Despite the shortcomings of the study, the device still has significant potential applications within the food industry for the advancements it has to offer.

References

- Bourne, Malcolm. *Food Texture and Viscosity: Concept and Measurement*. San Diego: Academic, 2002. Print.
- Boyar, M. M., and D. Kilcast. "Review food texture and dental science." *Journal of Texture Studies* 17.3 (1986): 221-52.
- Conserva, Enrico, Maria Menini, Tiziano Tealdo, Marco Bevilacqua, Francesco Pera, Giambattista Ravera, and Paolo Pera. "Robotic Chewing Simulator for Dental Materials Testing on a Sensor-Equipped Implant Setup." *International Journal of Prosthodontics* 21.6 (2008).

- Kress-Rogers, Erika, and Christopher Brimelow, eds. *Instrumentation and Sensors for the Food Industry*. 2nd ed. Boca Raton: Woodhead, 2001. Print.
- Lucas, P. W., J. F. Prinz, K. R. Agrawal, and I. C. Bruce. "Food Texture and Its Effect on Ingestion, Mastication and Swallowing." *Journal of Texture Studies* 35.2 (2004): 159-70.
- McGarry, J. "Design of a Fixture for Dynamic Evaluation of Forces During Mastication." Dissertation, unpublished. (2012)
- Meullenet, J-F. C., J. A. Carpenter, B. G. Lyon, and C. E. Lyon. "Bi-cyclical Instrument for Assessing Texture Profiles Parameters and Its Relationship to Sensory Evaluation of Texture." *Journal of Texture Studies* 28.1 (1997): 101-18.
- Meullenet, J-F. C., and J. Gross. "Instrumental Single and Double Compression Tests to Predict Sensory Texture Characteristics of Foods." *Journal of Texture Studies* 30.2 (1999): 167-80.
- Okiyama, S., K. Ikebe, and T. Nokubi. "Association between Masticatory Performance and Maximal Occlusal Force in Young Men." *Journal of Oral Rehabilitation* 30.3 (2003): 278-82.
- Peng, Yankun, Xiuzhi Sun, and Lin Carson. "Food Hardness and Fracturability Assessment by Electronic Sensing System." *Journal of Texture Studies* 33.2 (2002): 135-48.
- Rosenthal, Andrew J. *Food Texture: Measurement and Perception*. Gaithersburg: Aspen, 1999. Print.
- Sun, X. S., F. T. Wang, L. Carson, and C. Setser. "Electronic Sensing System for Food Texture Characterization." *Transactions of the ASAE* 44.3 (2001): 623-30.
- Szczesniak, Alina S., Margaret A. Brandt, and Herman H. Friedman. "Development of Standard Rating Scales for Mechanical Parameters of Texture and Correlation Between the Objective and the Sensory Methods of Texture Evaluation." *J. Food Science* 28.4 (1963): 397-403.

8.0 Conclusions

Peak forces measured by the fixture range from 7.95 N (Vermont cheddar) to 837.3 N (Ghirardelli 100% dark chocolate) in the normal direction and 0.530 N (dill Havarti) to 39.8 N (Ghirardelli 100% dark) in shear. These forces fall within the range of maximum bite force recorded by other studies, which vary from 315 N to 909 N, though it should be noted these forces without force feedback. Maximum recorded normal force, by type of food tested, is 146 N (club cracker), 160 N (oat square), 12.8 N (dill Havarti), 7.95 N (Vermont cheddar), and 245 N (granny smith apple). Hardness of different chocolate types is examined extensively, and it is found that the average hardness of chocolates tested, in order of cacao content, are 382 N (Cadbury milk chocolate), 487 N (Lindt 70% dark), 553 N (Ghirardelli 72% dark), 496 N (Lindt 90% dark), and 568 N (Ghirardelli 100% dark). This agrees with our prediction that increasing cacao content will increase brittle behavior of the food, and therefore increase measured hardness. It should be noted that cacao content does not directly imply hardness, as different manufacturers of chocolate have different correlations between hardness and cacao content. For Lindt chocolate, this is found to be $y=0.4807x+453.09$, where y is the measured hardness (N) and x is the cacao content (%). For Ghirardelli chocolate the relation is $y=0.5418x+514.24$. From these equations it can be seen that the increment of hardness is 0.481 N/1% cacao for Lindt chocolate and 0.542 N/1% cacao in Ghirardelli chocolate. Based on the standard deviations measured [ranging from 10.16 N (Lindt 90%) to 86.91 N (Ghirardelli 100%)] it is impossible to determine cacao content from hardness measurements alone. However, t-tests show that it is possible to distinguish chocolate made by different manufacturers based on hardness alone, especially with future improvements to fixture precision. A correlation between fracture toughness measured by the Instron and area under the force-time curve ($r^2=0.9718$ for Lindt 70% dark) indicates internal validity of the fixture in that its results are corroborated by the Instron, which is assumed to be correct. This procedure also allows for calculation of relative fracture toughness based on data produced by the fixture.

The fixture designed here enables its user to generate texture profiles for brittle and lightly viscoelastic foods as perceived by a human. Characteristic curves for a range of foods demonstrate its versatility for use with these diverse materials. It is possible to describe the nature of a food's texture based on the force applied to it by the teeth, and therefore how it is experienced in the mouth. With brittle foods including crackers and cold cereals, the fixture is able to distinguish between larger individual fractures and measure smaller fractures en masse during grinding. The nature of these materials makes it easy to relate visual qualitative data during a test to numerical data compiled and analyzed afterwards. Statistical analysis also shows that it is possible to differentiate chocolate produced by different manufacturers. These materials provide the highest level of clarity and consistency between tests, which has resulted in their use for most of the analysis. The fixture's capabilities are limited in distinguishing cacao content of chocolate, however, due to the minute increment of hardness with increasing content. Further studies may be capable of refining the sensitivity, developing new metrics for distinguishing content, and minimizing experimental error.

Testing has also brought to light potential improvements for the fixture. The strain rate and sensory resolution available while testing highly viscoelastic materials has proven inadequate for their

accurate measurement. Improvements to the strain rate will better model the deformation of these materials during mastication, and improvements to the data collection system will allow for more precise analysis of the smaller forces applied to these and all food samples.

Overall the concept of using the fixture for product discrimination is feasible based on the results of this study, although future refinements must be made. Correlation with sensory panel data would help to corroborate the data generated by the fixture, and indicate that it is an accurate representation of human perception. This would further validate the simplifications made and ensure that the method used is appropriate. The efficacy of the fixture for use within the food industry has been elucidated here, and it can be concluded that it has significant potential applications for the advancements it has to offer.

9.0 Works Cited

- Terminologia Anatomica*. (1998). Retrieved March 9, 2012, from Federative International Programme on Anatomical Terminologies: <http://www.unifr.ch/ifaa/>
- (2011). Retrieved March 9, 2012, from Texture Technologies: <http://www.texturetechnologies.com/texture-analysis/Probes-Fixtures.php>
- (2012). Retrieved from Pressurex: <http://www.pressurex.com/index.php>
- Anderson, D. (1956). Measurements of stress in mastication. *Journal of Dental Research*, 175-189.
- Bourne, M. C. (1968). Texture Profile of Ripening Pears. *Journal of Food Science*, 223-226.
- Calderon, P. d., Kogawa, E. M., Lauris, J. R., & Conti, P. C. (2006). The influence of gender and bruxism on the human maximum bite force. *Journal of Applied Oral Science*.
- Conserva, E., Menini, M., Tealdo, T., Bevilacqua, M., Pera, F., Ravera, G., et al. (2008). Robotic Chewing Simulator for Dental Materials Testing on a Sensor-Equipped Implant Setup. *International Journal of Prosthodontics*, 501-508.
- Conserva, E., Menini, M., Tealdo, T., Bevilacqua, M., Ravera, G., Pera, F., et al. (2009). The Use of a Masticatory Robot to Analyze the Shock Absorption Capacity of Different Restorative Materials for Prosthetic Implants: A Preliminary Report. *International Journal of Prosthodontics*, 53-55.
- Daumas, B., Xu, W., & Bronlund, J. (2005). Jaw mechanism modeling and simulation. *Mechanism and Machine Theory*, 821-833.
- G.D., W., & Williams, J. (1981). Gnathodynamometer: measuring opening and closing forces. *Dental Update*, 239-50.
- Gibbs, C. H., Mahan, P. E., Lundeen, H. C., Brehnan, K., Walsh, E. K., Sinkewiz, S. L., et al. (1981). Occlusal forces during chewing-Influences of biting strength and food consistency. *Journal of Prosthetic Dentistry*, 561-567.
- Hayashi, T., Kato, S., Nakajima, S., Yamada, Y., & Kobayashi, H. (1999). Physiological control scheme of jaw simulator JSM/2A for improving reproducibility of open-close movement. *Proceedings of the First Joint BMES/EMBS Conference*, (p. 564). Atlanta.
- Helkimo, E., & Ingervall, B. (1978). Bite force and functional state of the masticatory system in young men. *Swedish Dental Journal*, 167-175.
- Henry, W. F., Katz, M. H., Pilgrim, F. J., & May, A. T. (1971). Texture of Semi-solid Foods: Sensory and Physical Correlates. *Journal of Food Science*, 155-161.
- Kamegai, T., Tatsuki, T., Nagano, H., Mitsuhashi, H., Kumeta, J., Tatsuki, Y., et al. (2005). A determination of bite force in northern Japanese children. *European Journal of Orthodontics*, 53-57.

- Kawashima, K., Miura, H., Kato, H., Yoshida, K., & Tanaka, Y. (2009). The study of comminution behavior of food on buccal and lingual side during mastication. *Journal of Medical Dental Science*, 131-8.
- Martin, R. A. (1997, December 24). *The Power of Shark Bites*. Retrieved 2011, from Biology of Sharks and Rays: http://www.elasmo-research.org/education/topics/r_bites.htm
- Mello, P. C., Coppede, A. R., Macedo, A. P., Chiarello de Mattos, M. d., Rodrigues, R. C., & Ribeiro, R. F. (2009). Abrasion wear resistance of different artificial teeth opposed to metal and composite antagonists. *Journal of Applied Oral Science*.
- Mochizuki, Y. (2001). *Texture Profile Analysis*. Current Protocols in Food Analytical Chemistry.
- Orchardson, R., & MacFarlane, S. H. (1980). The effect of local periodontal anaesthesia on the maximum biting force achieved by human subjects. *Archives of Oral Biology*, 799-804.
- Ortuğ, G. (2002). A new device for measuring mastication force (Gnathodynamometer). *Annals of Anatomy*, 393-396.
- Osborn, J. (1996). Features of human jaw design which maximize the bite force. *Journal of Biomechanics*, 589-595.
- Regalo, S. C., Santos, C. M., Vitti, M., Regalo, C. A., de Vasconcelos, P. B., Mestriner, W., et al. (2008). Evaluation of molar and incisor bite force in indigenous compared with white population in Brazil. *Archives of Oral Biology*, 282-286.
- Rosenthal, A. J. (1999). *Food Texture: Measurement and Perception*. Gaithersburg: Aspen Publishers.
- Salles, C., Tarrega, A., Mielle, P., Maratray, J., Gorria, P., Liaboeuf, J., et al. (2007). Development of a chewing simulator for food breakdown and the analysis of in vitro flavor compound release in a mouth environment. *Journal of Food Engineering*, 189-198.
- Sun, C., Brolund, J., Huang, L., Morgenstern, M., & Xu, W. (2008). A Linkage Chewing Machine for Food Texture Analysis. *International conference on Mechatronics and Machine Vision in Practice*, (pp. 299-304). Auckland.
- Szczesniak, A. S., Brandt, M. A., & Friedman, H. H. (1963). Development of Standard Rating Scales for Mechanical Parameters of Texture and Correlation Between the Objective and the Sensory Methods of Texture Evaluation. *Journal of Food Science*, 397-403.
- Takanbu, H., Takanishi, A., & Kato, I. (1993). Design of a mastication robot mechanism using a human skull model. *Intelligent Robots and Systems*, 203-208.
- Takanobu, H., Takanishi, A., & Kato, I. (1993). Design of a Mastication Robot Mechanism Using a Human Skull Model. *IEEE/RSJ International Congress on Intelligent Robots and Systems*, (pp. 203-208). Yokohama.

- Takanobu, H., Yajima, T., Nakazawa, M., Takanishi, A., Ohtsuki, K., & Ohnishi, M. (1998). Quantification of masticatory efficiency with a mastication robot. *Robotics and Automation*, 1635-1640.
- Takanobu, H., Yajima, T., Nakazawa, M., Takanishi, A., Ohtsuki, K., & Ohnishi, M. (1998). Quantification of Masticatory Efficiency with a Mastication Robot. *IEEE Conference of Robotics & Automation*, (pp. 1635-1640). Leuven.
- Tanzawa, T., Futaki, K., Tani, C., Hasegawa, T., Yamamoto, M., Miyazaki, T., et al. (2011). Introduction of a robot patient into dental education. *European Journal of Dental Education*, 195-199.
- Torrance, J., Pap, J.-S., Xu, W., Brolund, J., & Foster, K. (2006). Motion control of a chewing robot of 6 RSS parallel mechanism. *Proceedings of International Conference on Autonomous Robotics and Agents*, (pp. 12-14). Palmerston North.
- Van Der Bilt, A., Tekamp, A., Van Der Glas, H., & Abbink, J. (2008). Bite force and electromyography during maximum unilateral and bilateral clenching. *European Journal of Oral Sciences*, 217-222.
- Van Steenberghe, D., & de Vries, J. H. (1978). The influence of local anaesthesia and occlusal surface area on the forces developed during repetitive maximal clenching efforts. *Journal of Periodontal Research*, 270-274.
- Villamil, M. B., Nedel, L. P., Freitas, C. M., & Maciel, A. (2005). A Model to Simulate the Mastication Motion at the Temporomandibular Joint. San Diego: International Society for Optical Engineering.
- Waltimo, A., & Könönen, M. (1993). A novel bite force recorder and maximal isometric bite force values for healthy young adults. *European Journal of Oral Sciences*, 171-175.
- Waltimo, A., & Könönen, M. (1995). Maximal bite force and its association with signs and symptoms of craniomandibular disorders in young Finnish non-patients. *Acta Odontologica Scandinavica*, 254-258.
- Woda, A., Mishellany-Dutour, A., Batier, L., Francois, O., Meunier, J.-P., Reynaud, B., et al. (2010). Development and validation of a mastication simulator. *Journal of Biomechanics*, 1667-1673.

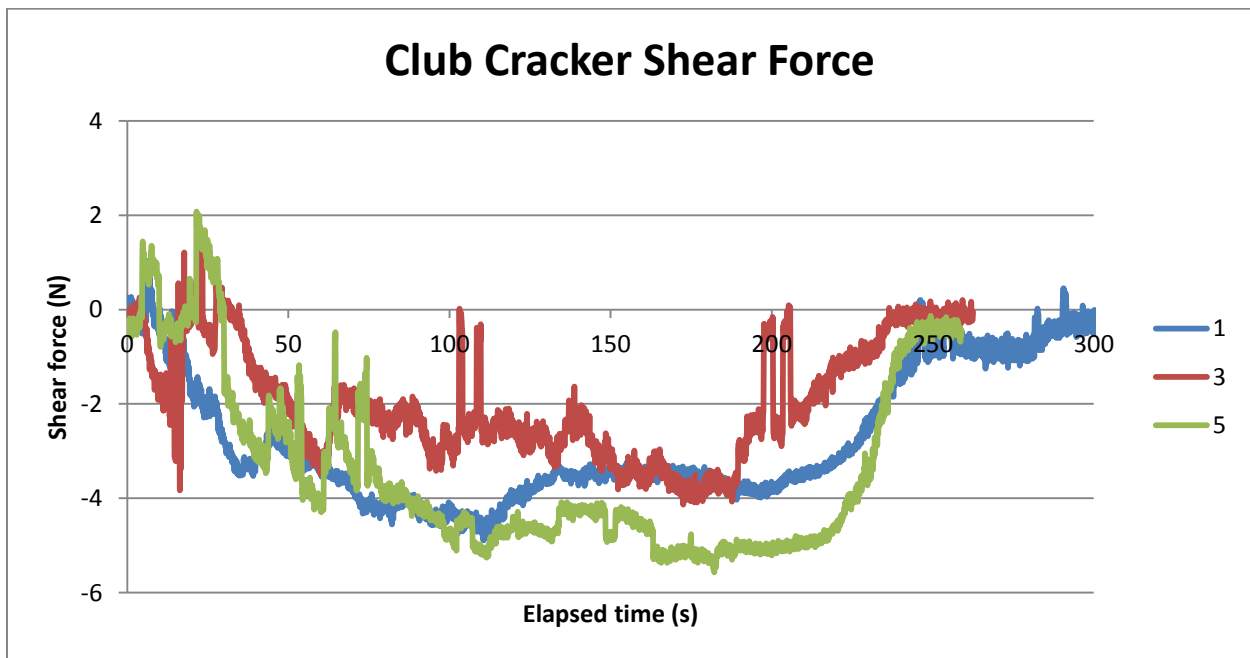
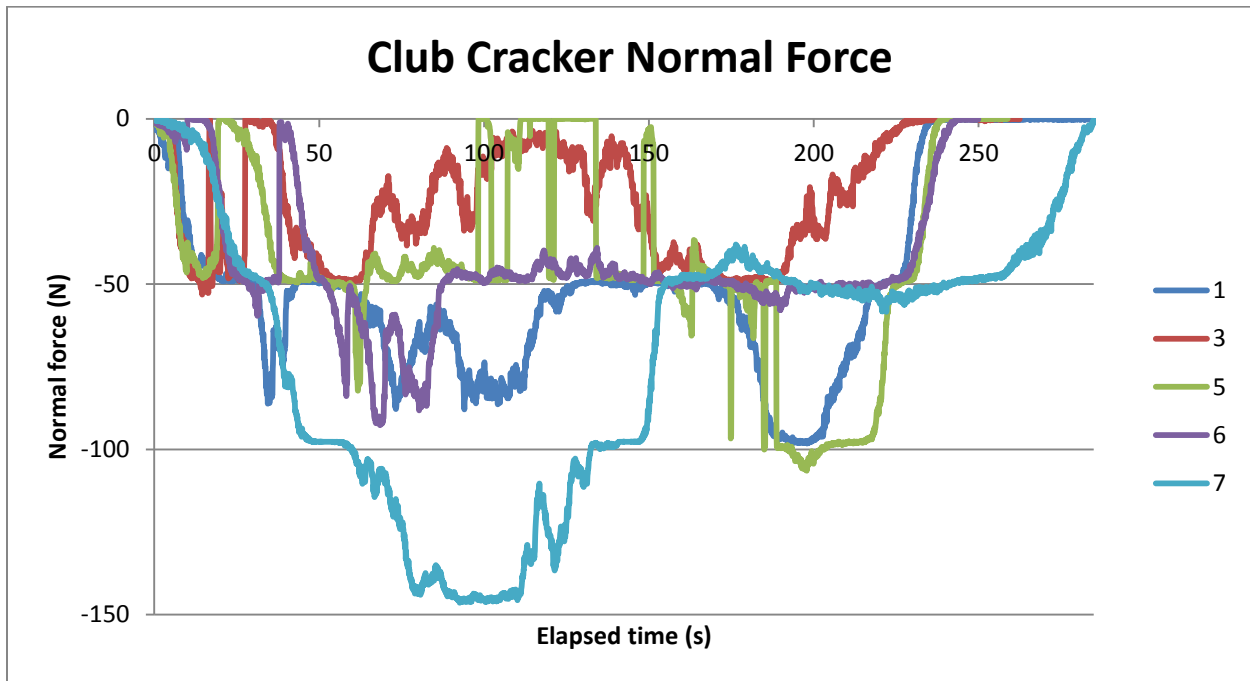
10.0 Appendix

Experimental data collected by both the fixture and corroboratory information gathered by the Instron program is presented here. A summary of sample preparation and testing methods is presented first to distinguish differences in sample testing.

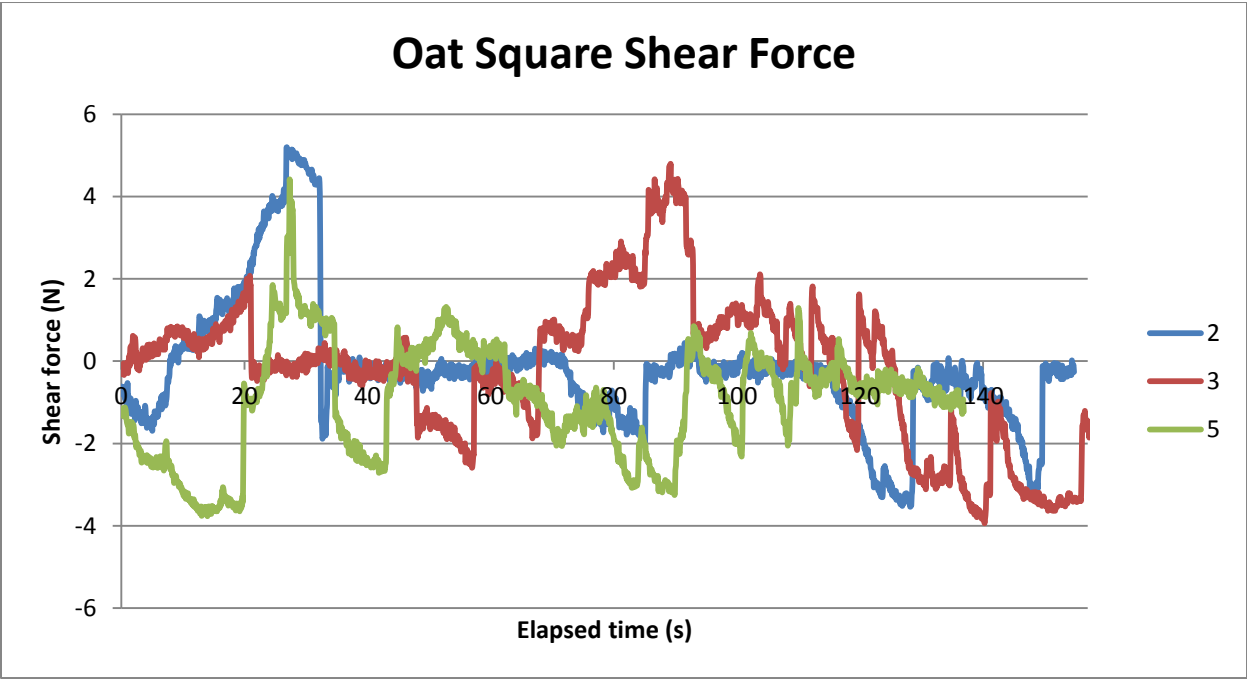
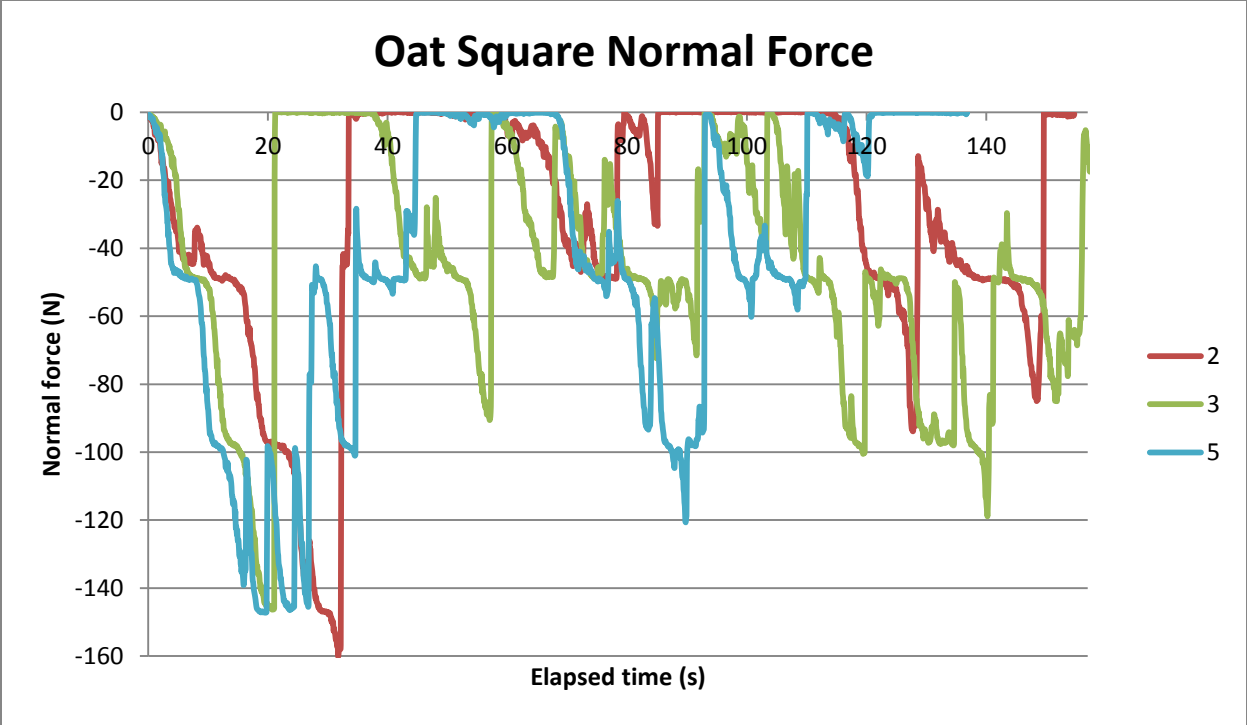
Food	Brand	Food Type	Preparation	Crosshead Speed
Club Cracker	Keebler	Brittle	None	10 mm/min
Oat Square	Quaker	Brittle	None	10 mm/min
Dill Havarti Cheese	Boar's Head	Highly Viscoelastic	14 mm cube	10 mm/min
Vermont Cheddar	Cabot	Highly Viscoelastic	14 mm cube	10 mm/min
Granny Smith apple	N/A	Lightly Viscoelastic	14 mm cube	10 mm/min
Milk Chocolate	Cadbury	Lightly Viscoelastic	None	10 mm/min
70% Dark Chocolate	Lindt	Lightly Viscoelastic	1 x 2.5 cm pc.	100 mm/min
72% Dark Chocolate	Ghirardelli	Lightly Viscoelastic	1 x 2.5 cm pc.	100 mm/min
90% Dark Chocolate	Lindt	Lightly Viscoelastic	1 x 2.5 cm pc.	100 mm/min
100% Dark Chocolate	Ghirardelli	Lightly Viscoelastic	1 x 2.5 cm pc.	100 mm/min

Across all data sets, the normal force refers to a force applied along the intersection of sagittal and coronal planes. Negative force indicates compression of the sample and positive force is sample adhesion (tension). The shear force is applied along the intersection of sagittal and transverse planes and a negative shear refers to positive displacement along the top of the sample (maxillary surface) and negative displacement along the bottom (mandibular surface). Sample numbers do not necessarily count sequentially with some foods because data may have been improperly acquired or lost. No data has been excluded in situations where data was recorded that did not fit the experimental model. Force data acquired for brittle foods (including crackers and oat square cereal pieces) is presented first, beginning with Keebler Club Crackers.

10.1 Brittle Foods

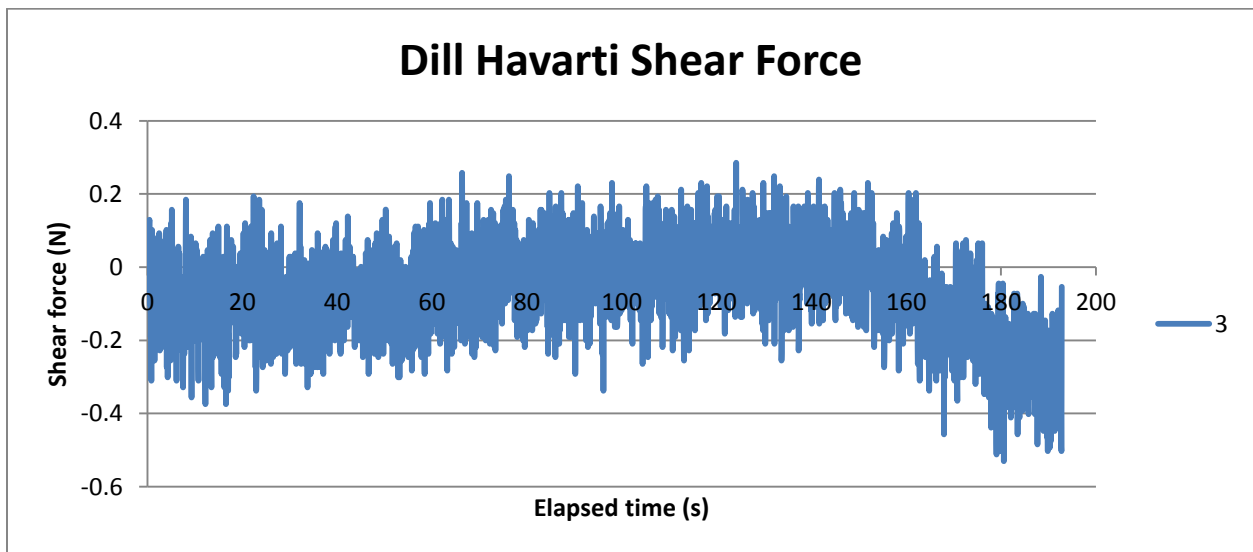
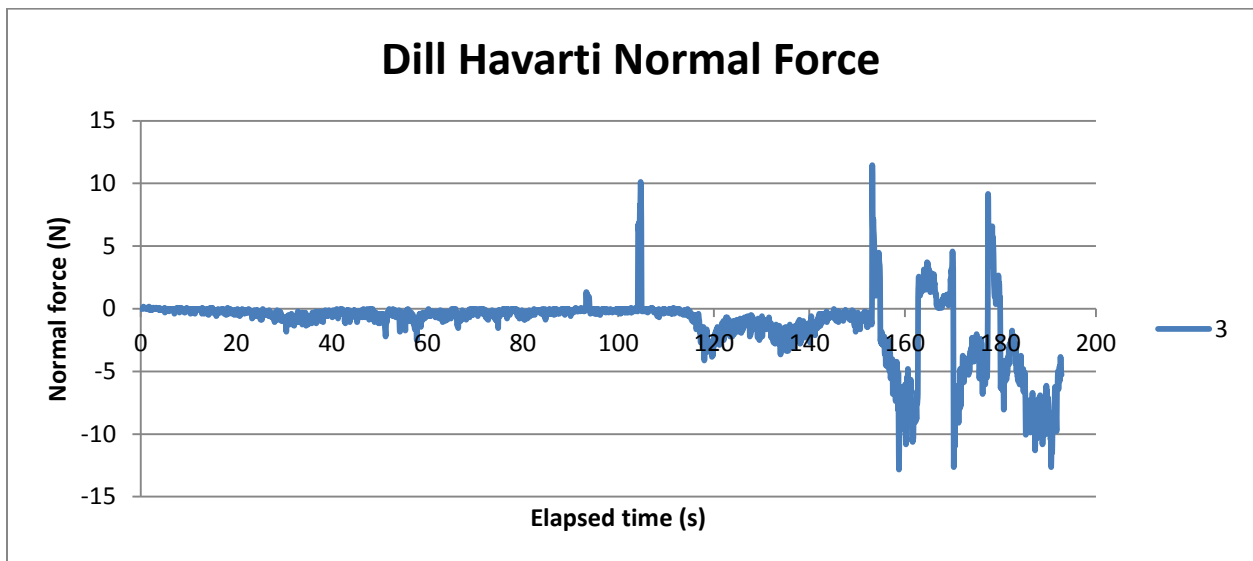


Shear force data for sample numbers 6 and 7 was lost and is excluded. Sharp peaks and “saw-tooth” shapes are generally indicative of samples breaking, but without falling out of the fixture. Noticeable breaks (visually or audibly so) are recorded by the experimenter to correlate significant breaks with the data. Data for Quaker Oat Squares follows.

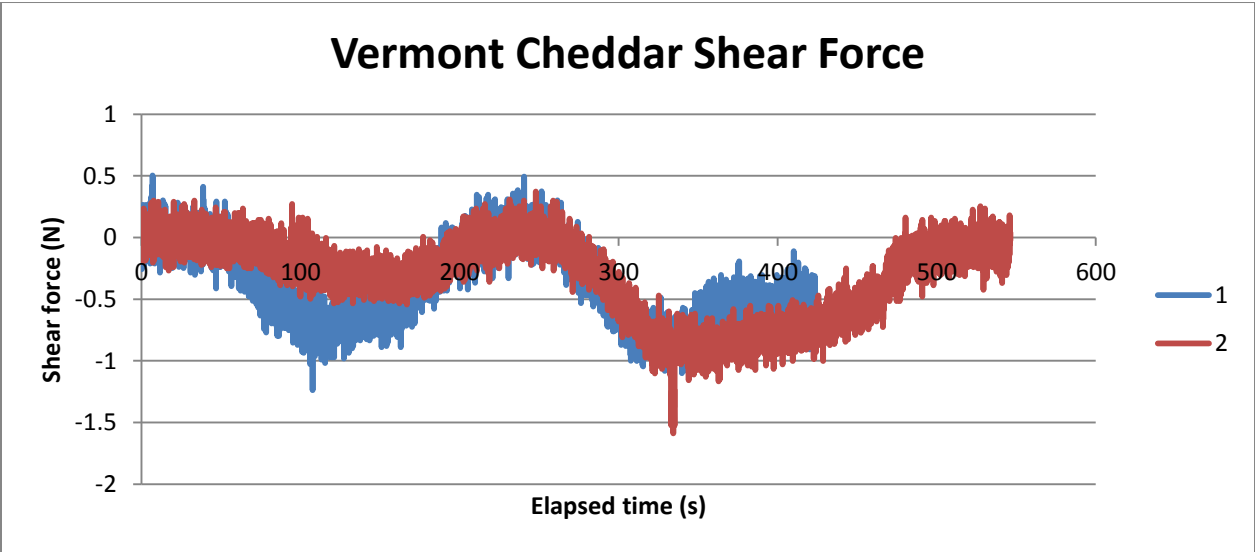
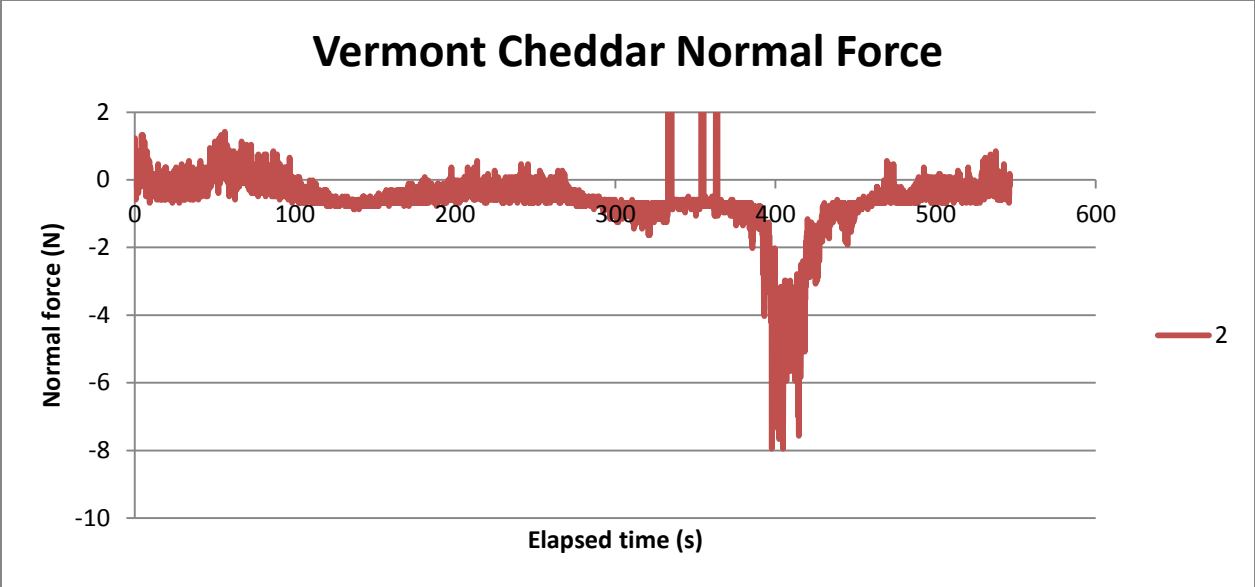


Similarly to the club crackers, these brittle cereal pieces fracture repeatedly with “sawtooth” shapes that indicate sample breakage. Data presentation continues with highly viscoelastic foods, beginning with Boar’s Head Dill Havarti.

10.2 Highly Viscoelastic Foods

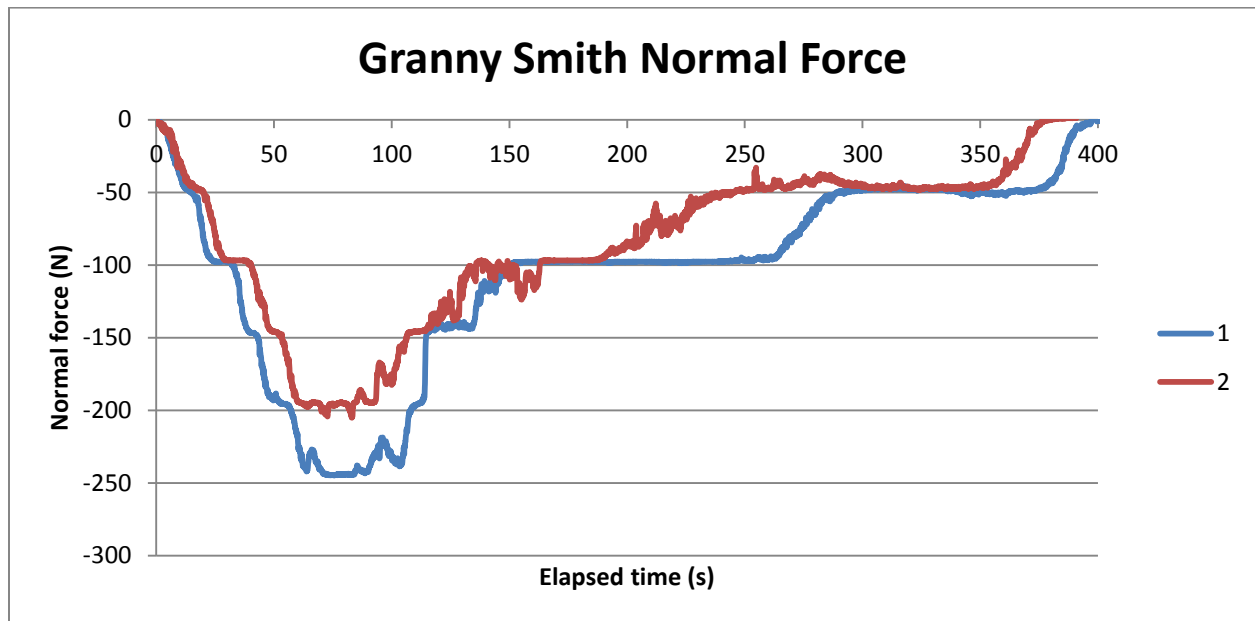


Very few samples of highly viscoelastic foods were tested at this cross-head speed because viscous behavior dominates at this speed. Furthermore, the fixture's data acquisition is much noisier at this low level of force, as seen in the shear force. The shear data is provided here only to indicate that it is insufficient. Several sharp peaks are seen in the normal force that do not represent food texture, but aberrant noise. Similar data is seen for subsequent highly viscoelastic foods continuing with Cabot Vermont Sharp Cheddar.

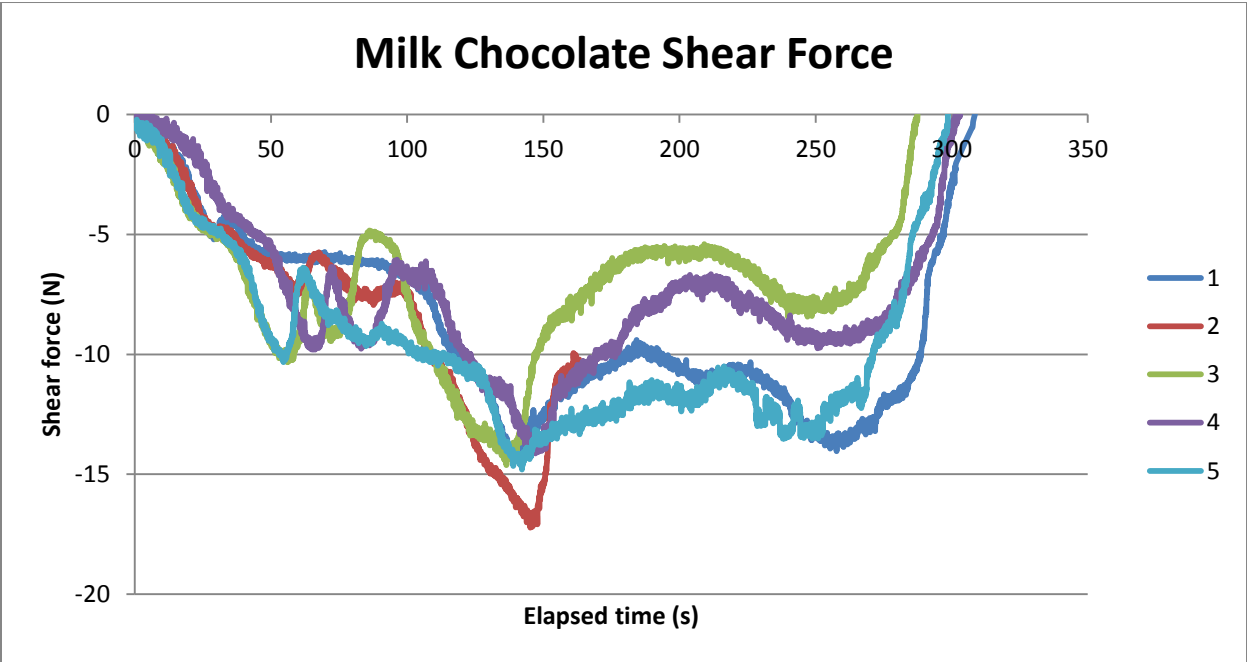
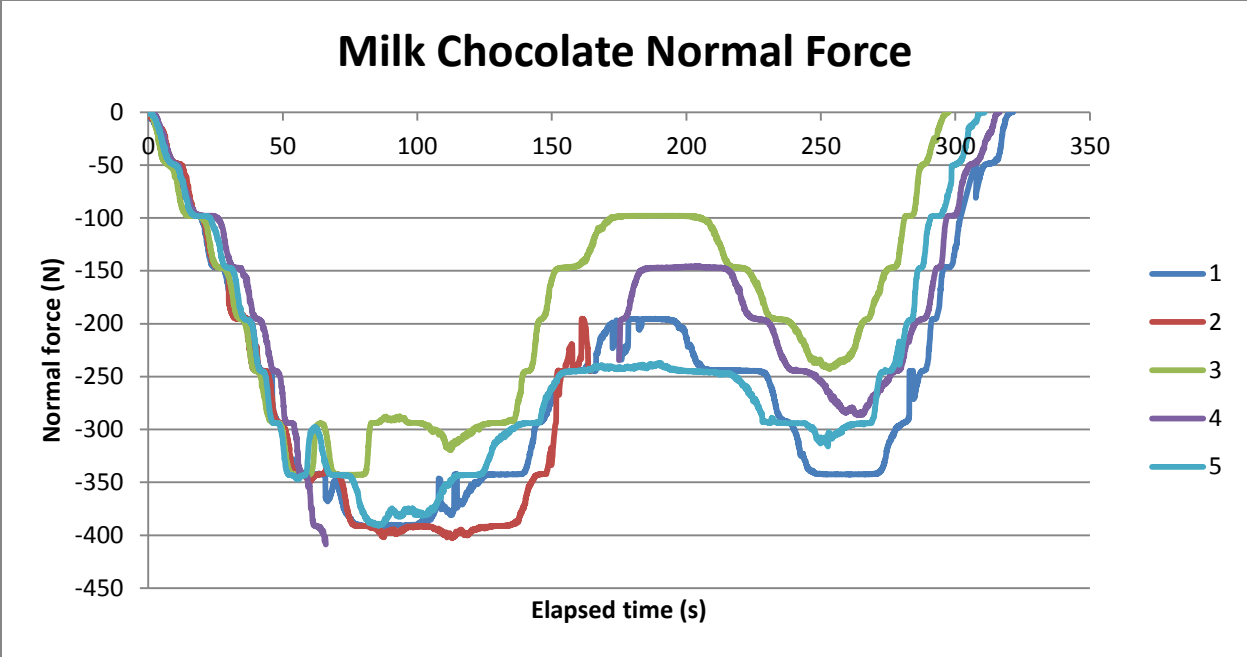


Normal force data for sample 1 was obscured by transient electrical noise and is not included. Both data sets are still noisy at this level of force application but are still representative of the applied force. Food groupings continue with lightly viscoelastic foods beginning with granny smith apples.

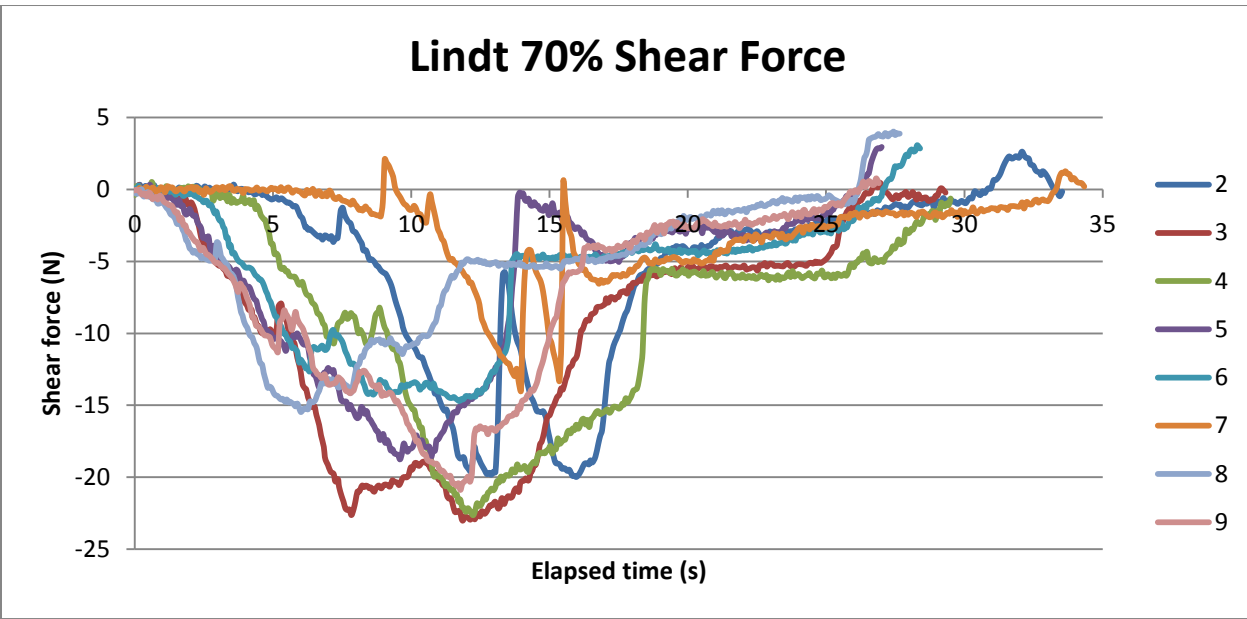
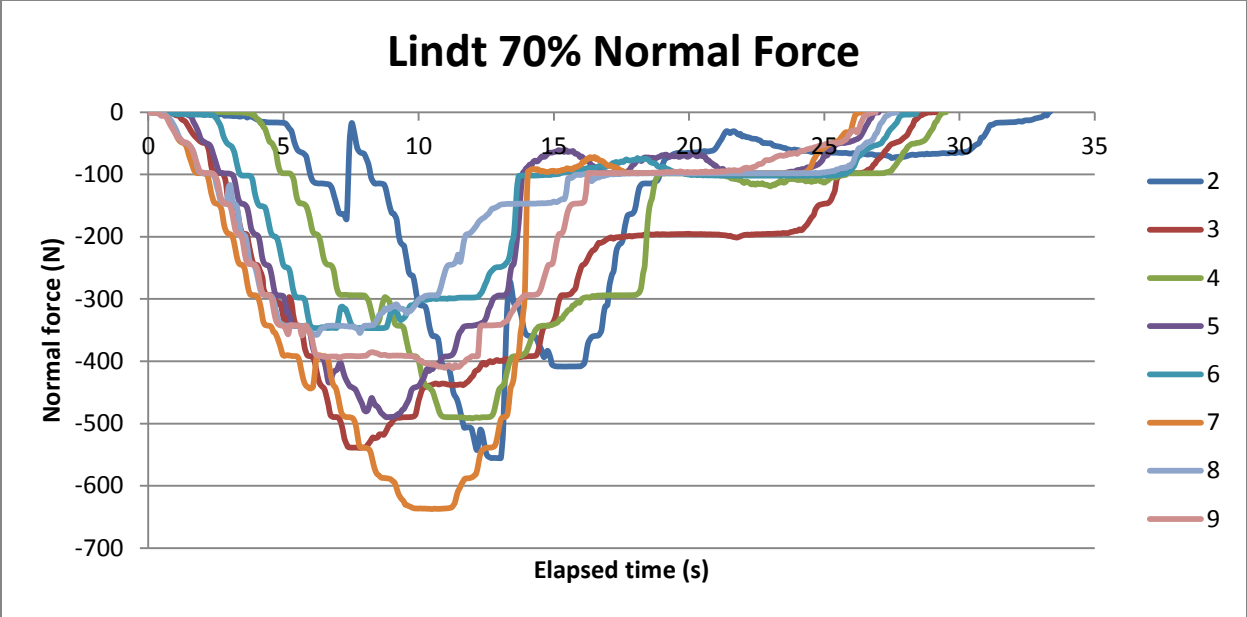
10.3 Lightly Viscoelastic Foods



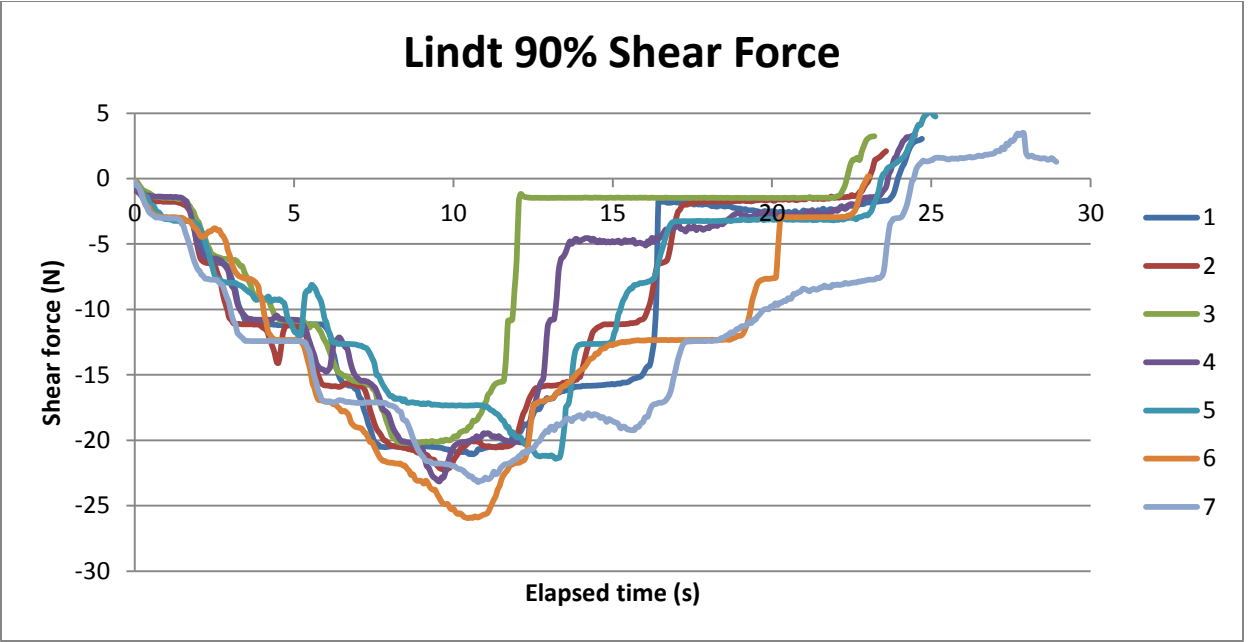
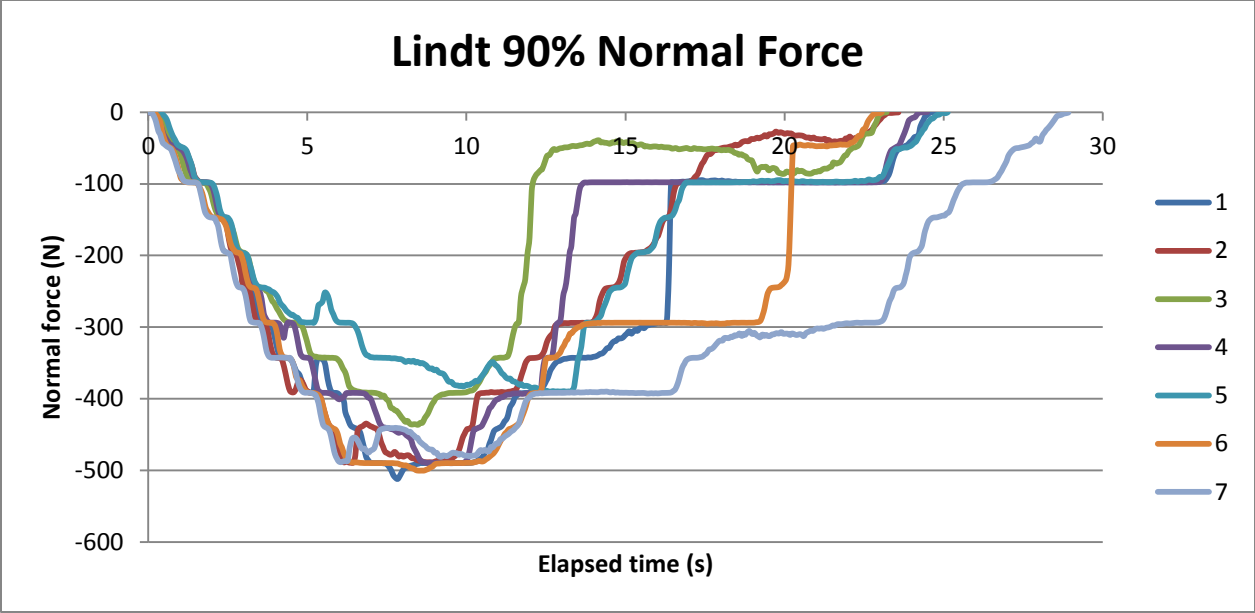
Shear force data for the apples was lost and is not included here. There is less noise in the apple data because they are significantly less viscous than samples such as cheese, which will flow under an applied stress. Apples are considered to be lightly viscoelastic here because of the solid cellular structure (elastic component) and juices (viscous component). The remaining data sets describe the texture of different chocolate types starting with milk chocolate.



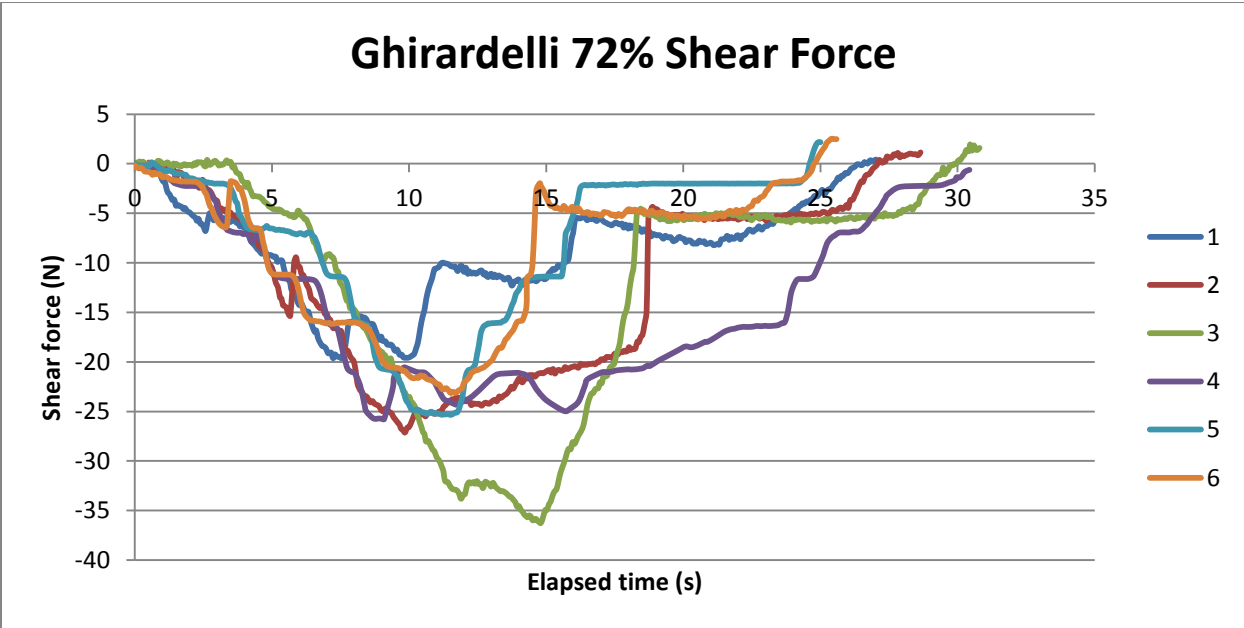
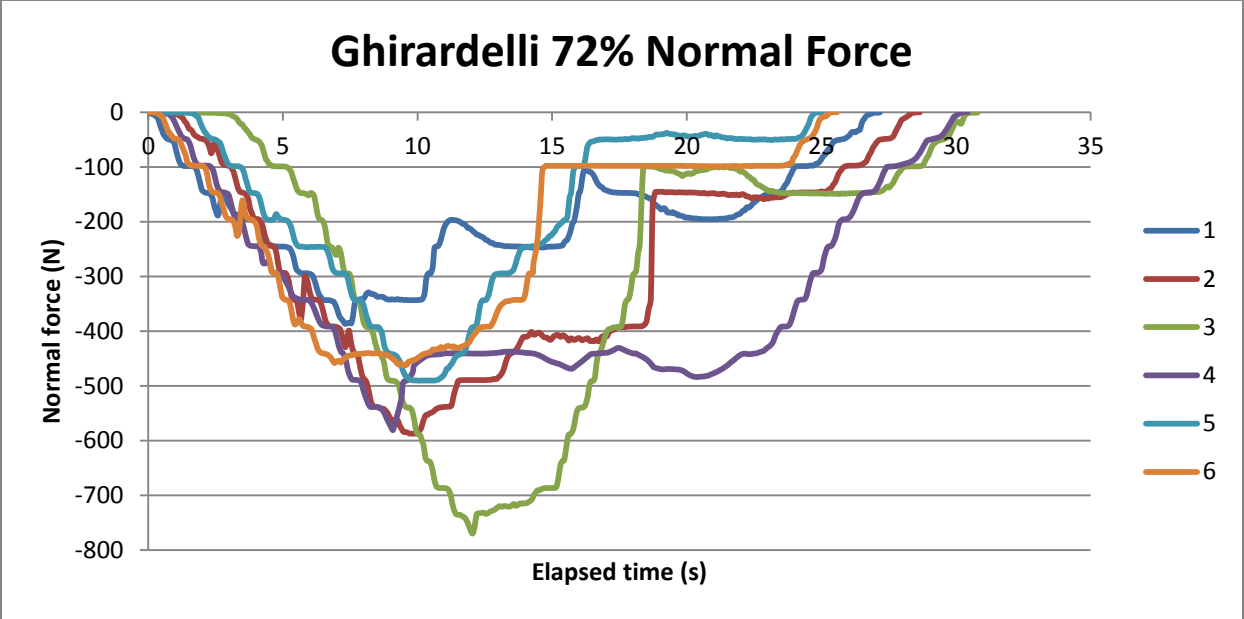
Some normal force data was lost for sample 4 because of transient electrical noise, and a portion of data between time $t=66$ s and $t=175$ s was removed. Testing for sample 2 was aborted at $t=165$ s because of electrical noise that disrupted the remainder of the test run. This is the only chocolate type that was tested at 10 mm/min and with whole pieces (squares cut from a chocolate bar). All subsequent dark chocolate pieces are tested at 100 mm/min to increase testing efficiency and with samples cut from individual chocolate squares to minimize waste. The first of these dark chocolate samples is Lindt 70% Dark chocolate.



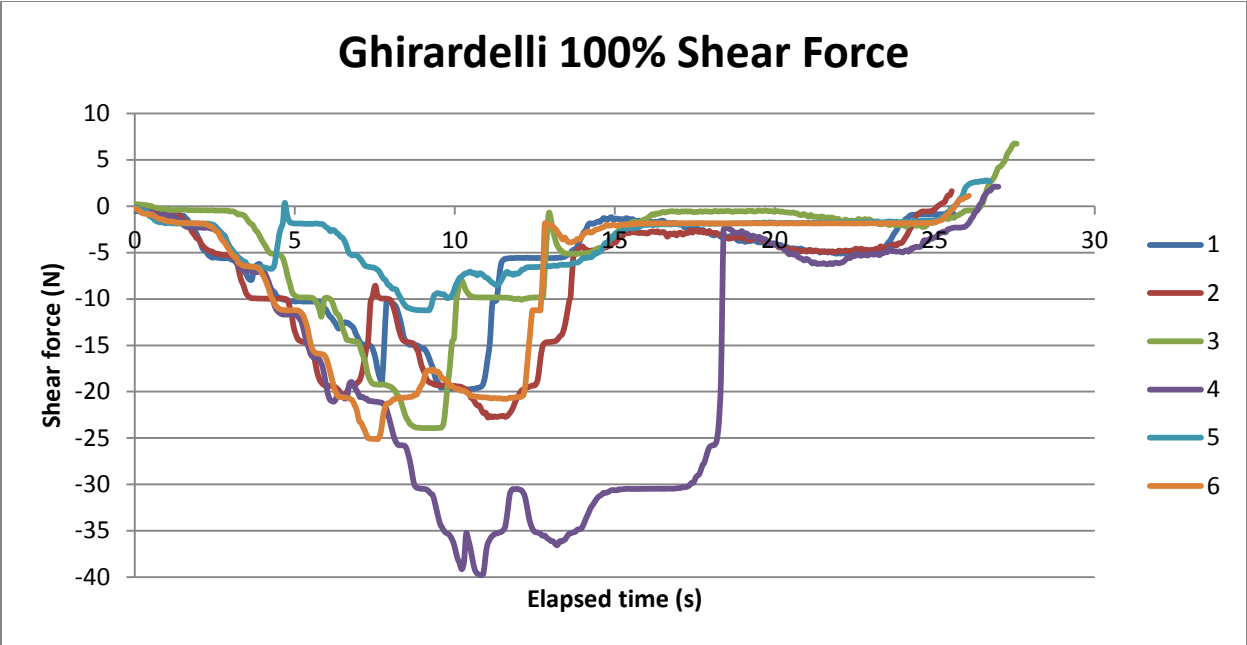
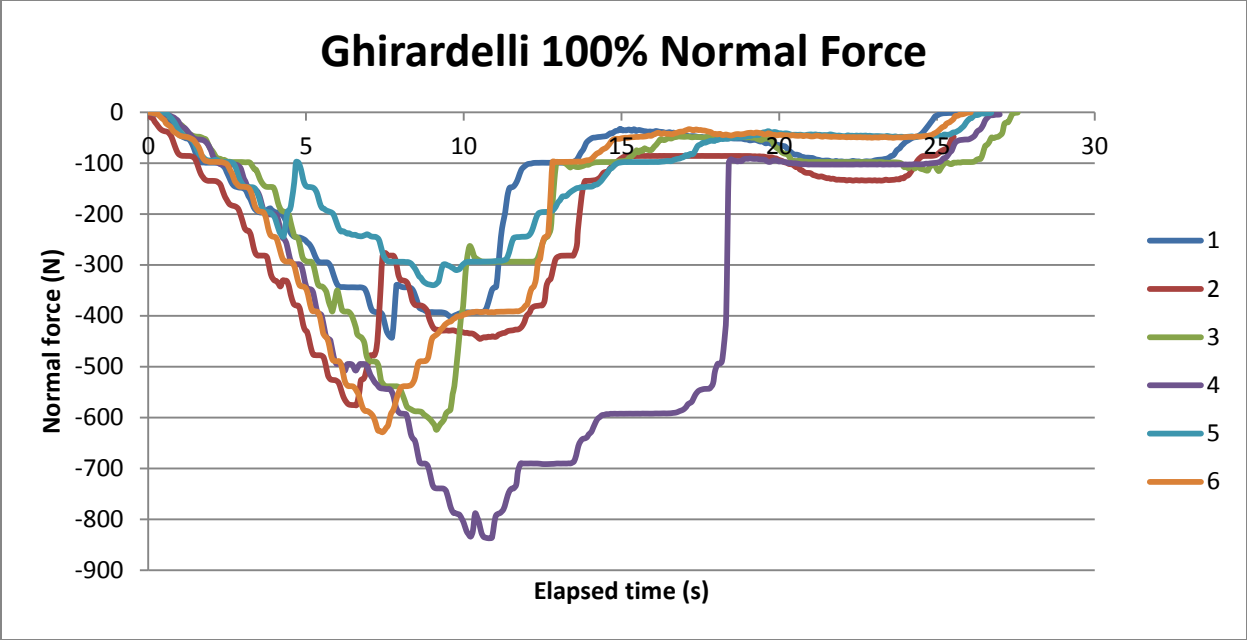
Samples two and four are offset because of slippage of the sample within the fixture. Sample 7 has an aberrant hardness and shear texture profile because a piece of the sample broke off and lodged between teeth 6 and 27 (incisors). The 70% dark chocolate has the lowest cacao content of the four samples of dark chocolate tested. This is followed by Lindt 90% cacao chocolate.



The data gathered for the 90% dark chocolate is the most precise of all data sets, as indicated by the close grouping of the set of curves. Samples 3 and 5 slipped during testing and therefore did not attain the maximum possible force. Ghirardelli chocolates of similar cacao content follow, beginning with 72% dark.



Sample 1 slipped during testing and did not reach the appropriate force peak. Samples 2, 3, and 4 show some of the effects of sample pieces breaking off and lodging between the top and bottom incisors. The final chocolate selection is Ghirardelli 100% dark chocolate.



Samples one, two, and five slipped during testing and failed to maximize the contact area. Test four is exaggerated because of a broken piece that was stuck between the incisors.

10.4 Sample Masses

Masses of each sample tested, average mass, and standard deviation are tabulated here. All masses are given in grams.

Sample	1	2	3	4	5	6	7	8	9	Avg	StDev
Cracker	3.37	3.36	3.42	3.42	3.25	3.31	3.36	-	-	3.356	0.060
Cheddar	3.42	3.49	-	-	-	-	-	-	-	3.455	0.049
Havarti	3.52	-	-	-	-	-	-	-	-	3.52	-
Apple	3.12	2.91	3.01	-	-	-	-	-	-	3.013	0.105
Milk Choc.	5.32	5.62	5.45	5.71	5.49	5.66	-	-	-	5.542	0.147
70% Dark	2.76	2.52	2.51	2.40	2.51	2.57	2.49	2.33	2.23	2.48	0.151
72% Dark	3.03	2.94	3.10	2.71	2.70	-	-	-	-	2.896	0.183
90% Dark	2.57	2.41	2.30	2.60	2.57	2.41	2.31	-	-	2.453	0.127
100% Dark	3.37	3.29	3.20	3.27	3.25	3.17	-	-	-	3.258	0.071